AN ABSTRACT OF THE THESIS OF

Florian G. Bell for the degree of Doctor of Philosophy in Physics presented on January 7, 1986 .

Title: Optical Absorption in Liquid Semiconductors .

Redacted for Privacy

Abstract approved: _____ .

Melvin Cutler

An infrared absorption cell has been developed which is suitable for high temperature liquids which have absorptions in the range .1 - 10^3 cm^{-1}. The cell is constructed by clamping a gasket between two flat optical windows. This unique design allows the use of any optical windows chemically compatible with the liquid. The long-wavelength limit of the measurements is therefore limited only by the choice of the optical windows. The thickness of the cell can easily be set during assembly, and can be varied from 50μm to .5 cm.

Measurements of the optical absorption edge were performed on the liquid alloy $Se_{1-x}Tl_x$ for x = 0, .001, .002, .003, .005, .007, and .009, from the melting point up to 475°C. The absorption was found to be exponential in the photon energy over the experimental range from 0.3 eV to 1.2 eV. The absorption increased linearly with concentration according to the empirical relation $\alpha_T(h\nu) = \alpha_1 + \alpha_2 x$, and the

absorption α_1 was interpreted as the absorption in the absence of Tl. α_1 also agreed with the measured absorption in 100% Se at corresponding temperatures and energies. The excess absorption defined by $\Delta\alpha=\alpha_T(h\nu)-\alpha_1$ was interpreted as the absorption associated with Tl and was found to be thermally activated with an activation energy E_t=0.5 eV.

The exponential edge is explained as absorption on atoms immersed in strong electric fields surrounding ions. The strong fields give rise to an absorption tail similar to the Franz-Keldysh effect. A simple calculation is performed which is based on the Dow-Redfield theory of absorption in an electric field with excitonic effects included. The excess absorption at low photon energies is proportional to the square of the concentration of ions, which are proposed to exist in the liquid according to the relation $C_i \propto x^{1/2} e^{-E_t/kT}$, which is the origin of the thermal activation and the proportionality to Tl concentration.

The ionic model satisfactorily explains the observed concentration and temperature dependence of the absorption. It also provides for the first time, a universal explanation of the exponential edge in liquid semiconductors where charged defects are present, and provides a means of measuring the concentration of ions when the absorption can be calibrated.

Optical Absorption in Liquid Semiconductors

by

Florian G. Bell

A Thesis
submitted to
Oregon State University

in partial fulfillment of
the requirements for the
degree of

Doctor of Philosophy

Completed January 7, 1986

Commencement June 1986

APPROVED:

Redacted for Privacy

Professor of Physics in charge of major

Redacted for Privacy

Chairman of Department of Physics

Redacted for Privacy

Dean of Graduate School

Date thesis is presented January 7, 1986

Typed by Florian G. Bell for Florian G. Bell

ACKNOWLEDGEMENTS

During my work I was fortunate to be able to draw upon the experience and encouragement of supportive people who went beyond their duty in helping me. Of those, first, I would like to express thankfulness for my wife Drinda, whose love, encouragement, and help were unending. I would like to acknowledge her help in preparing many of the graphs.

I cannot estimate the countless hours spent by my patient mentor, Professor Melvin Cutler, in challenging me to be a good scientist. I am very fortunate to have been able to work with him and benefit from his expertise in research.

Acknowledgements go to Professors Alan Wasserman and Henri Jansen for helpful discussions, and to Professor John Gardner for his help while my advisor was on leave. I was fortunate to have as a reference the thesis of Henri Rasolondramanitra on transport properties of liquid semiconductors.

I would like to remember my friend and teacher, the late James Ballenger, and to thank my brother Patrick, who both introduced me to physics. I am grateful to those of my family who gave me moral support during my graduate years, especially the "Seattle Crew". I am also grateful for the financial support given by my wife's parents, Dr. and Mrs. Jack Davis, during the last year of this work. My many friends made sure I am more than a physicist: Paul Brunetto, Bill and Dawn Econe, Anne Fiedler, Peter Gumplinger, Bill and Kerri Irwin, Herbert and Ellen Jaeger, Alex Montgomery, Dan Mumbach, Jeff and Marie Schnick, Henri Rasolondramanitra, Irma Wright, and Wilbur are a few recent ones.

Finally, I would like to dedicate this thesis to the memory of my mother and father, two people of uncompromising courage and integrity who sacrificed so much for their children. They taught me the value of education.

This research has been supported by the National Science Foundation grant No. DMR 83-20547.

TABLE OF CONTENTS

LIST OF FIGURES

Figure | Page

LIST OF TABLES

OPTICAL ABSORPTION IN LIQUID SEMICONDUCTORS

1. INTRODUCTION

This thesis concerns the optical absorption edge in liquid semiconductors, in particular, measurement and analysis of the optical absorption edge in the selenium-thallium alloy system. Although the present work has been performed on a single system, the results of this investigation have broader implications on the general problem of optical absorption in liquid semiconductors, hence the title. In this introduction are described some general features of the liquid semiconductors and the optical absorption edge in liquid and amorphous semiconductors. The next chapter outlines the investigations which have been made in the past, while pointing out some unanswered questions that remain both theoretical and experimental challenges.

1.1 Liquid semiconductors

There are many molten alloys with semiconducting properties [9]. The present work will focus on the liquid element selenium or a liquid alloy containing the elements selenium or tellurium as at least one component. These two elements belong to the group VIB, which are called the *chalcogens*. Selenium will be referred to throughout the following as the liquid semiconductor prototype.

The chemical structure of selenium and tellurium are similar. The

outer shell contains four electrons in p-states. Two of the electrons are paired in a σ_p state and form the so-called lone-pair (non-bonding) orbital. The two remaining electrons form covalent bonds, giving rise to a two-fold bonded atom in the fully coordinated crystals. Structurally, trigonal selenium and tellurium are also similar. The individual atoms are bonded in the crystalline state in spiral chains, with two nearest neighbors. The chains are arranged parallel to one another along the c-axis to form a hexagonal lattice [27]. The nearest-neighbor (intrachain) distance is smaller, corresponding to a covalent bond distance, than the second-nearest neighbor (interchain) distance [27,28,60]. The inter-chain bonds are therefore weaker. There is also theoretical evidence from the pressure dependence of the band edges in trigonal Se [24] and experimental evidence from the pressure dependence of Raman scattering in trigonal Se [2] that the intra-chain bonds are stronger than the inter-chain bonds. Therefore, upon melting, the inter-chain bonds weaken, allowing some retention of the chains in the liquid state. The length of chains decreases with temperature [20], and this is apparent in the decreasing viscosity of selenium as the temperature is raised [3,20,21].

Crystalline Se also exists in another form, the monoclinic structure. In this form, Se atoms covalently bond in closed 8-fold rings with alternating dihedral angles in the ring. The rings stack along the c-axis. It is believed that small concentrations of Se_8 rings also exist at low temperatures in the liquid state; this concentration may decrease with increased temperature [4,22]. The experimental evidence for the

existence of rings in liquid Se is fairly ambiguous at this time [54].

In the amorphous and liquid forms of these two-fold (2F) coordinated materials, it is possible for deviations from the normal coordination to occur. When the chains are terminated at finite lengths, chain ends result. These one-fold (1F) centers can be either neutral or negatively-charged. The neutral atoms are sometimes called "dangling bond atoms" and are paramagnetic. The neutral centers are designated C_1^0, and the negatively-charged centers, correspondingly, C_1^-. In addition to chain ends, there also exist three-fold (3F) centers which are usually positive and designated C_3^+. A 3F bond atom can capture an electron and become neutralized, and is then designated as C_3^0. The positive 3F bond atom is favored energetically over the neutral 3F bond atom. To obtain electrical neutrality, charged defects must be formed of opposite sign in equal numbers. When the concentration of defects is high enough, the defects C_3^+ and C_1^- may form in close pairs, termed "intimate valence alternation pairs" by Kastner [61]. It is believed that the formation of these pairs can be represented by the reaction:

$$2C_1^0 \rightarrow C_3^+ + C_1^-, \qquad (1.1)$$

which may be exothermic [26], but this is uncertain. The formation of ions has immediate implication to the optical absorption spectrum of liquid semiconductors, as will be proposed in Chapter 5.

The bonding defects just mentioned are not unique to the lone-pair elements, but are more easily formed on chalcogen atoms. This is because the the non-bonding orbitals are available to reconfigure the bonding by placing electrons into antibonding orbitals as well as bonding orbitals. The resulting differences in energies of the different bond atoms are discussed in detail by Kastner [12] and by Vanderbilt and Joannopoulos [13]. The defects form localized states in small concentrations and narrow bands in larger concentrations, which are within the normal energy band gap, that is, within the gap defined by the valence band and the anti-bonding σ^* band. When the concentration of the defect states becomes appreciable, changes appear in the electronic behavior of the materials. These changes can be readily seen, for example in the conductivity and thermopower of the alloys $Se_{1-x}Te_x$ and $Se_{1-x}Tl_x$, where electronic transport occurs in an acceptor band forming within the gap as the concentration x or the temperature increases [11,14,15]. Although one might expect defect state bands to appear in optical absorption studies as well, there is no direct evidence that they do. This will be discussed in the next chapter.

In a liquid alloy containing the chalcogens, one expects all of the above mentioned defects to be present, but with different concentrations. In fact, the different defects do occur, with the normal 2F bond atoms predominating. At low temperatures, the concentrations of all other types are low, but the concentrations increase with temperature through thermal excitation. Amorphous alloys, on the other hand, will

tend to have constant concentrations of all types, since the atoms cannot move appreciably.

1.2 Optical absorption in liquid semiconductors

Selenium, whose conductivity at room temperature is extremely low (less than $10^{-13}\ \Omega^{-1}cm^{-1}$), is regarded as a semiconductor, due to the strong temperature dependence of its conductivity, and it has an optical band gap of the order 2 eV. Tellurium, on the other hand, is a borderline semiconductor, since it has a much higher conductivity (order $10^{3}\ \Omega^{-1}cm^{-1}$), and an optical band gap of .32 eV. Liquid alloys of the two elements show a continuous variation of the conductivity and thermoelectric power with concentration [1,11,14]. Upon melting, selenium retains its semiconducting properties. This is also true of many of its alloys such as with arsenic, and thallium. The conductivity is observed to change with temperature over many orders of magnitude in selenium and its alloys, reflecting the semiconducting behavior [1].

The conductivity and thermoelectric power of liquid semiconductors have been extensively studied. Because these properties are not of immediate interest to this work, the many investigations shall not be reviewed here. Instead, the interested reader is referred to the excellent books by Mott and Davis [7], Tauc [8], Cutler [9] and Brodsky [10], and the theses of Perron [1] and Rasolondramanitra [11] for full discussions. In addition to these properties, the authors review work on

magnetic susceptibility, x-ray scattering, neutron scattering and other topics. The concern here will be with the problem of optical absorption and related optical properties.

In the next chapter are listed the optical absorption studies on liquid semiconductors which have been made up to the present. As discussed there, the optical absorption edges in liquid Se, Se-Te, and As-Se alloys are observed to be exponential over the experimentally accessible regions of energy. The magnitude of the absorption coefficient at the lowest measureable photon energies (≈0.5 eV) is of the order 10^{-1}-10^{0} cm^{-1}, and the exponential behavior persists up to the highest measureable absorption levels, which are about 10^{3}-10^{4} cm^{-1} near 1 eV. The significance of this rule can be understood by considering that the band gap in crystalline Se is close to 2 eV. (The terms *band gap* and *optical band gap* will be used interchangeably.) The absorption coefficient can be represented by the empirical equation:

$$\alpha(h\nu) = A \exp[\gamma(h\nu - E_0)], \qquad (1.2)$$

where $h\nu$ is the photon energy and A is chosen so that α has the value for interband absorption at the band gap, which in this case is E_0. This exponential form of the absorption has, in the past, been referred to as the "Urbach rule," reminiscent of the absorption in alkali-halides. Urbach [55] first observed such an absorption in sensitivity measurements of photographic emulsions. Since then, exponential absorption has been

observed in a variety of materials, particularly the amorphous and liquid semiconductors. The reader is referred to the paper by Dow and Redfield [43] for a thorough discussion of Urbach's rule. Although the term "Urbach rule" has been widely used to refer to the exponential edge, it may also imply a definite temperature dependence to the absorption, which may not be an accurate representation in some materials. In Chapter 4 the Urbach rule will be discussed in more detail along with its implications to the interpretation of the data.

Although there is some deviation from the exponential rule at low absorption values and at low energies in some samples [1], its ubiquitous nature suggests that there is a common origin of it in all liquid semiconductors. There is no generally accepted explanation for the exponential rule, but several models have been proposed. These models are described in the next chapter.

1.3 Objectives of this work

The topic of this thesis is the optical absorption edge in the liquid semiconductors. In the hope that it would be possible to reveal the mechanism responsible for the exponential rule, systematic measurements have been made of the absorption edge in $Se_{1-x}Tl_x$. This system was chosen for several reasons. The element thallium is soluble in selenium over most of the composition and temperature range, the absorption increases continuously with Tl concentration, and the alloy is simple to prepare. In addition, conductivity and thermoelectric power

have been investigated in the Se-Tl system by Rasolondramanitra and Cutler [11,15], and they have derived values for the concentration of ionic species as a function of temperature and Tl concentration. The concentration of ions is an important consideration of the ionic model to be discussed in Chapter 5. As with other liquid semiconductors, the absorption was found to follow the exponential rule from $\alpha \approx .1$ cm^{-1} at $h\nu \approx .25$ eV up to $\alpha \approx 10^3$ cm^{-1} at $h\nu \approx 1.4$ eV. This rule was found to hold over all temperature ranges, and that has permitted a careful study of the effect of temperature, in addition to the effect of the photon energy.

The data obtained in this experiment have enabled the critical examination of several of the proposed models for optical absorption. In the next chapter these models will be described, with emphasis on the factors which can be experimentally examined. Also, in the next chapter are outlined the studies which have been made in the past on optical absorption. In the third chapter the experimental arrangement is described: the optical cell design and the optical layout used. In the fourth chapter the data are presented in several formats to illustrate the important results. The inconsistencies in the conventional interpretations of optical absorption in liquid semiconductors will be pointed out. In the fifth chapter a simple calculation is undertaken which relates the presence of charged defects to the expected absorption in an electric microfield, and the results will be compared to the data. The concept of an activation energy will also be introduced to explain the observed temperature dependence of the absorption coefficient as

measured in the alloy $Se_{1-x}Tl_x$. The thesis will be concluded with a discussion of the relationship between the model and the data and suggestions will be made for future work in this area.

2. BACKGROUND

2.1 Previous experimental work

To date, the amount of data obtained on optical properties of liquid semiconductors is scant. There are several reasons for this. First, the liquid semiconductors are toxic and corrosive, and that has placed severe limitations on the experimental methods. Second, they exist as liquids only at temperatures well above room temperature, and this leads to further experimental restrictions. Finally, the liquids all absorb light strongly in the visible, and have absorption coefficients as large as 100 cm^{-1} in the near infrared. This points out the need for a thin optical cell for absorption studies in the visible and near infrared. An important result of this work is the development of a thin absorption cell transparent to infrared light.

Table 2.1 lists the optical studies of liquid semiconductors which have been made up to the present. Direct structural studies such as Raman scattering and far infrared absorption have been omitted.

Table 2.1. Optical Studies of Liquid Semiconductors (Abbreviations: OA, Optical Absorption; PC, Photoconductivity; R, Reflectivity; and TE, Thermal Emissivity)

Investigator [Ref.]	Date	System	Type of Study
Caldwell and Fan [28]	1959	Se	OA
Hodgson [6]	1963	Te	R
Edmond [5]	1966	As_2Se_3, As_2SeTe_2	OA
Siemsen and Fenton [19]	1967	Se	OA
Tauc and Abraham [17]	1968	CdTe	TE
Perron [1]	1969	Se, Se-Te	OA
Rabit and Perron [16]	1973	Se	OA, PC
Trotter, et al. [29]	1978	Ga-Te, In-Te, Tl-Te	R
Fainschtein and Thompson [18]	1980	Se-Te	R

Early absorption work in liquid selenium was included in the paper of Caldwell and Fan [28] on optical properties of crystalline Se and Te. Transmission was measured in liquid Se in the range .6 μm to 2 μm, and infrared absorption was measured in liquid Se at 493 K. In the work of Hodgson [6], reflectivity was measured in liquid Te at 500 and 600°C

from 430 nm to 2.5 μm. Edmond [5] measured the optical absorption edge in As_2Se_3 thin films, and absorption at longer wavelengths in the liquid at temperatures from 288 °C up to 597 °C. The absorption in the liquid state was interpreted as free-carrier absorption. The optical absorption was found to be exponential in the photon energy ($h\nu$) in the thin films and nearly exponential in the range interpreted as a free-carrier regime. Siemsen and Fenton [19] also found that the absorption in pure Se is exponential in $h\nu$ at all temperatures studied, up to 400 °C, from $h\nu$=.5 eV to $h\nu$=2.0 eV. Tauc and Abraham [17] measured thermal emissivity in a quartz cell containing liquid CdTe, and compared it to the known emissivity for liquid Ge. In this way, the reflectivity of the CdTe-quartz interface was obtained from

$$R_q(h\nu) = 1 - \epsilon(h\nu), \tag{2.1}$$

where ϵ is the emissivity. The reflectivity found in this way showed an increase with $h\nu$ at 1 eV, in contrast to the theoretically expected result for free carrier absorption.

The most extensive previous study of absorption in a liquid semiconductor system was undertaken by Perron [1] in $Se_{1-x}Te_x$ alloys for x=0, .1, .2, .3, .5 from room temperature up to 500 °C. Perron found that the absorption was nearly exponential in the energy from $h\nu$=.5 eV to $h\nu$=1.5 eV over all temperatures and concentrations. In addition, the

absorption was found to increase continuously with tellurium concentration. These effects were interpreted in terms of an increase of the density of localized states within the band gap (see band-tailing model below) and a shift of the band gap to lower energies with temperature and concentration. For liquid selenium, Perron found that the data followed an empirical the relationship:

$$\alpha(h\nu)=\alpha_0 \exp[a(h\nu-E_k(T))], \tag{2.2}$$

and

$$a(T)= -1.57 + 6.81\times10^{3}/T \ eV^{-1}. \tag{2.3}$$

The parameter $E_k(T)=E_{k0}-E_{k1}T$, so if the absorption data are plotted as $\ln \alpha$ vs. 1000/T (Arrhenius plot), an essentially linear relationship results. Also, this empirical rule implies that the slope of such plots will have a linear relationship to $h\nu$, in keeping with the Urbach rule (The Urbach rule is discussed in Section 1.2. The present measurements of the absorption in liquid Se do not show such a linear relationship, and this will be discussed in detail in Chapter 4.).

The measurement of reflectivity in liquid semiconductors has been of limited value for two reasons. First, it is not easy to identify significantly sharp features which would give definite indication of the shape of energy bands. Also, a Kramers-Kronig analysis to determine the optical constants is difficult, due to the need for reflectivity data at other than optical frequencies. In spite of these limitations, Thompson

and co-workers [29,18] have used reflectivity to infer the dielectric functions in several liquid semiconductors.

It is possible to determine the index of refraction directly from reflectivity measurements when the absorption is known. In particular, Fainchtein and Thompson [18] have measured reflectivity in Se-Te alloys up to 500 °C in a sapphire cell. They have used these measurements along with the absorption as measured by Perron [1] to obtain the index of refraction. The index of refraction for liquid Se determined in this way has been very valuable for the present work.

2.2 The optical absorption problem

In order to understand the problem of optical absorption in liquid semiconductors, let us compare the optical absorption edge in liquid selenium to that in amorphous and crystalline selenium. Figure 2.1 shows the optical absorption edge in crystalline (trigonal and α-monoclinic) [33], amorphous (room temperature) [24], and liquid selenium [19]. The absorption coefficient is plotted in units of cm^{-1}. As described in Chapter 1, crystalline Se exists in either of two forms. If, as suggested in the literature, we consider that amorphous Se is composed of a mixture of chain and ring structures, analagous to the trigonal and monoclinic structures [22], then it is not surprising that the absorption edge in the amorphous form is intermediate between the two edges of the crystalline forms. This is consistent with the belief that the general features of the density of states are determined by short-range order, and

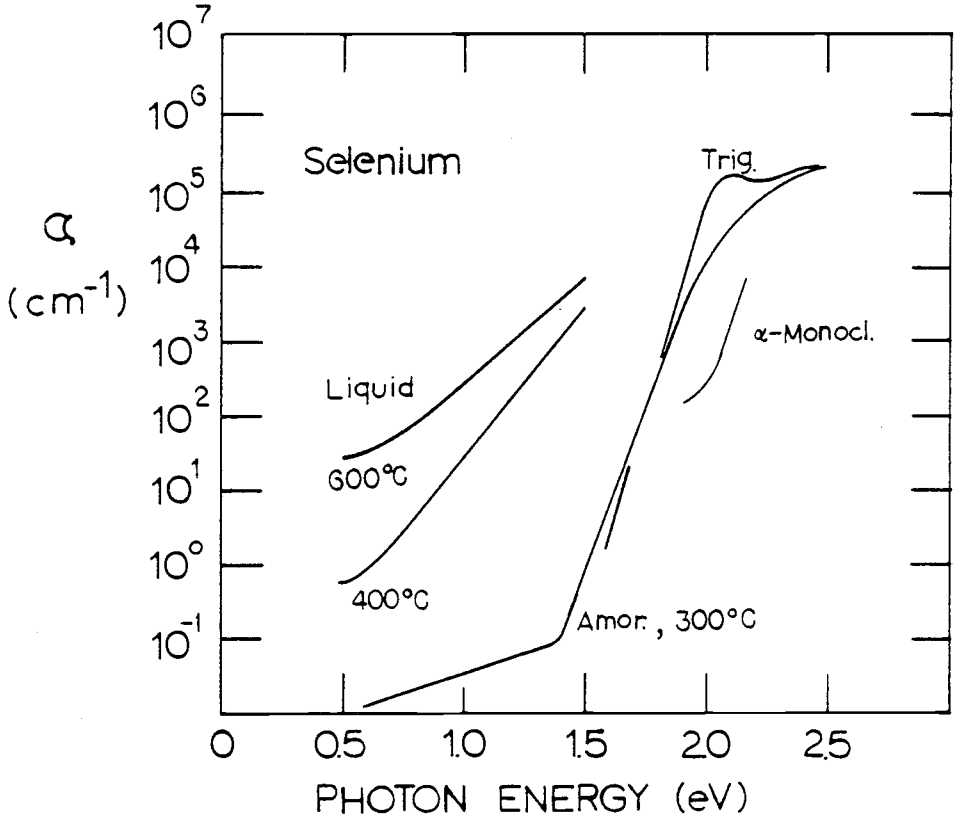

Figure 2.1 Optical absorption in selenium from Ref. 19, 24, and 33.

that short-range order is mostly preserved in the amorphous state [30]. Therefore we expect the optical band gap to be similar in the crystalline and amorphous forms. In the liquid state, the edge is shifted in the long wavelength direction. A widely accepted interpretation of this has been that the optical band gap is smaller in the liquid state and decreases with increasing temperature.

The terms *band gap* and *optical band gap* have been used loosely. Let us now consider what is exactly meant by the band gap in an amorphous or liquid semiconductor. In a crystalline semiconductor, the optical band gap can be defined as the minimum energy required to excite an electron initially at the top of the valence band to the lowest lying state in the conduction band. Absorption coefficients measured at the onset of optical absorption in crystals are likely to be as large as 10^5 cm^{-1}. The optical band gap in the crystalline forms of Se is around 2 eV [23].

Now in an amorphous or liquid semiconductor, there is no well-defined band gap. It is therefore customary to take the energy at which the absorption coefficient has some arbitrarily large value to be the band gap. Customarily, this has been taken to be 10^3 cm^{-1} for the liquid semiconductors, as higher absorption values can not be directly measured. The choice of a higher absorption value, say comparable to that appropriate for interband transitions in crystalline Se, demands that the experimental absorption curves be extrapolated to obtain the energy E_g. If the optical band gap is taken to be where the optical

absorption is $\approx 10^5$ cm^{-1}, then it is found that this energy is around 2.0 ev in amorphous and liquid selenium, corresponding to the value in the crystal.

A less arbitrary way to establish the optical band gap is to take E_g to be the energy at which photoconductivity "turns on," i.e., where the efficiency for photoconductivity approaches unity. By measuring the efficiency of photoconductivity, Hartke and Regensburger [24] were able to separate the absorption in amorphous Se into photoconductive and nonphotoconductive parts. Figure 2.2 shows the results of their investigation. The photoconductive contribution to the absorption begins at about 2.0 eV with an absorption of 10 cm^{-1} and increases to 10^4 cm^{-1} at 2.4 eV If we consider the efficient process above 2 eV to be interband transitions, then this energy is a reasonable value for the optical band gap.

A similar situation exists in liquid selenium. In Figure 2.3 we show the results of optical absorption and photoconductivity measurements in liquid selenium at 230 °C as reported by Rabit and Perron [16,62]. The solid curve is the normalized photocurrent, which is proportional to the quantum efficiency. It increases continuously below 2.0 eV and begins to approach a constant value at 2.2 eV. These data would seem to indicate that a band gap of 2 eV should be taken for the liquid and amorphous forms of Se. However, there is considerable absorption for energies down to at least .5 eV, and $\alpha \approx 100$ cm^{-1} at 1 eV.

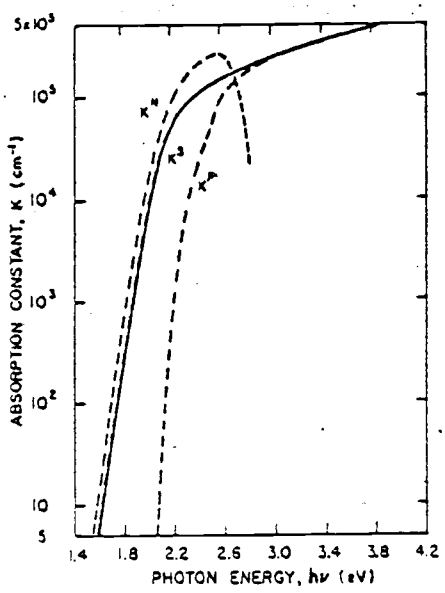

Figure 2.2 Optical absorption in amorphopus selenium resolved into photoconductive and nonphoto-conductive parts. From Ref. 24.

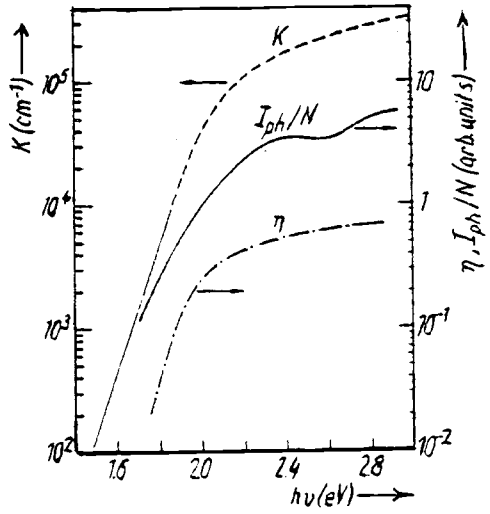

Figure 2.3 Optical absorption and efficiency of photo-conductivity in liquid selenium at 230 °C. From Ref. 16.

The studies of Perron and of Siemsen and Fenton outline the general problem of optical absorption in liquid semiconductors. There is an unexplained large absorption at energies less than what we can regard as the optical band gap. The absorption is nearly exponential in the photon energy and it is seen to increase with temperature as $\ln \alpha = A + B/T$. In the case of alloys of Se with Te and with metallic elements, the absorption increases with the concentration of the metallic element. Let us now turn to the discussion of some models which have been proposed to explain this phenomenon.

2.3 Theoretical models

2.3.1 The band tailing model

Let us begin the discussion by considering an optical absorption model which we shall call the band tailing model, and is due to Tauc [8]. It is based on a density of states picture similar to that of Cohen, Fritzsche, and Ovshinsky [30] (the CFO model). This model is schematically represented in Figure 2.4. In this model, it is assumed that the semiconductor has a density of states that consists of extended valence and conduction states which are separated by a *mobility gap*. Extended states within the conduction band terminate abruptly at the conduction band *mobility edge* (E_{mc}) Extended states within the valence band terminate at the valence band mobility edge (E_{mv}). The optical band gap itself is defined as the difference in energy between the

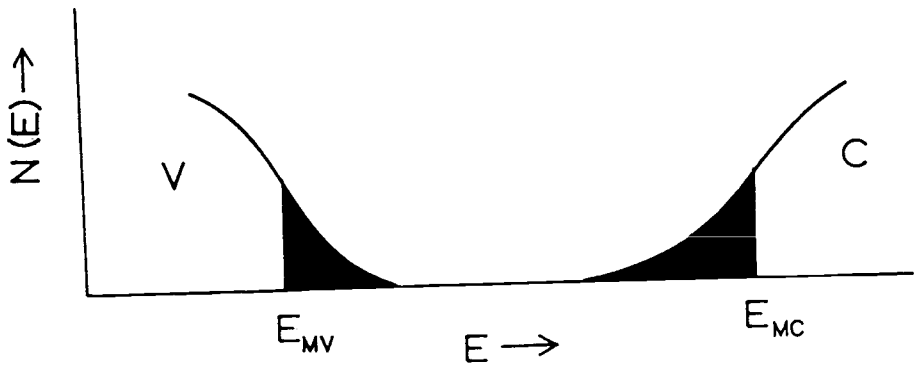

Figure 2.4 Density of states for a disordered system in the "band-tailing" model.

conduction band mobility edge and the valence band mobility edge. Within the gap are localized states that tail into the gap continuously. It is assumed that optical transitions occur which connect filled, extended states in the valence band with empty, localized states at the bottom of the conduction band. The opposite kind of transitions, from localized states in the valence band to extended states in the conduction band, is also possible. Transitions between localized states are not expected to give rise to significant absorption, due to the negligibly small overlap of the wave functions. A mathematical expression for the absorption coefficient due to transitions between localized and nonlocalized states has been derived by Hindley [31] and by Mott [32]. It is:

$$\alpha(h\nu) = \frac{8\pi^2 e^2 a^3 p^2}{3m^2 \omega n c} \int g_V(E) \cdot g_C(E+h\nu) dE \ , \qquad (2.4)$$

where g_V and g_C are the densities of states in the valence and conduction bands, $h\nu=\hbar\omega$ is the photon energy, a is the volume per unit cell, n is the index of refraction, and p is an average momentum matrix element for the transition, which we may assume to be constant. In this model, the absorption is proportional to the joint density of states of the conduction and valence bands. If it is assumed that the extended states form a parabolic band and that the localized states form an exponential tail, the shape of the exponential remains after the integration, giving an

absorption which is exponential in $h\nu$. Such a calculation can be easily done, and it implies a fairly large density of localized states throughout the mobility gap.

One obvious result of this model is that the temperature dependence may only be accounted for by an increase in the density of localized states, or by a shift of the band gap to lower energies. The density of localized states is, indeed, expected to increase with temperature, but the exact temperature dependence is unknown. In addition, this model requires a large density of states throughout the band gap, exponentially decreasing with energy from the mobility edge [47].

There is another objection to the band tailing model. This model predicts that there should be optical absorption resulting from transitions between extended states in the bands and localized states in the gap. Therefore, one should be able to detect the localized states through optical absorption. In addition, the shape of the absorption coefficient should reflect the folded density of states. Now the work of Rasolondramanitra and Cutler [11,14] has shown that there is a narrow band of acceptor states which forms within the gap in the liquid alloy system $Se_{1-x}Te_x$, for x=.3 to .5. Perron [1] has measured the optical absorption in these alloys up to x=.5, but there is no indication of such a band in the optical absorption shape. The only reasonable conclusion is that the absorption in these states, if present, is masked by a stronger absorption process, which cannot be accounted for by this model.

2.3.2 The band shift model

In the past, the increase in absorption with temperature has been interpreted as a shift of the edge to lower energies as the temperature increases. Although a shift of the band gap is an attractive hypothesis, it is not entirely consistent with the data. Consider, for example the absorption edge in liquid selenium as reported by Siemsen and Fenton [19] and Rabit and Perron [16]. The results of the work of Siemsen and Fenton are shown in Figure 2.5. A value can be obtained for the band shift $\Delta E/\Delta T$ by plotting the energy corresponding to a particular absorption value vs. temperature (isoabsorption curves). Shifts obtained in this way are -.0027 eV/°C for α=10, -.0020 eV/°C for α=100, and -.0014 eV/°C for α=1000 cm^{-1}. The shifts uniformly decrease with increasing α, and the projected shift becomes zero at a value of $\alpha \approx 1.3 \times 10^5$ cm^{-1}, as can be seen in Figure 2.5. The energy at this projected absorption is 2 eV. Now one would expect that if the band gap were undergoing a real shift, it would be uniform for *all* absorption values, and this is not the case. This interpretation of the absorption shift therefore seems dubious.

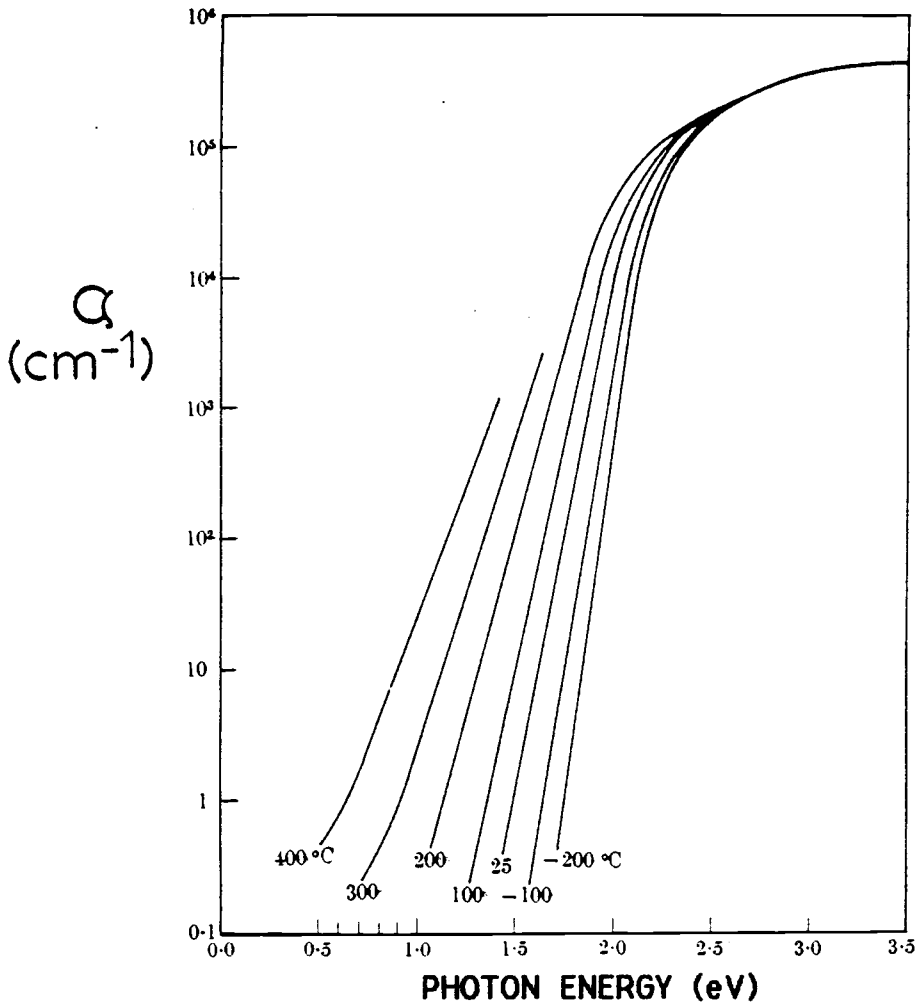

Figure 2.5 The optical absorption edge in amorphous and liquid selenium. From Ref. 19.

2.3.3 The electric microfield model

The next model to be described is based on the Franz-Keldysh effect, or electroabsorption [34-40]. The diagram of Figure 2.6 illustrates this effect. It is known that when a crystalline semiconductor is placed in an externally applied uniform electric field, the energy bands are tilted in space. In this case, transitions can occur for photon energies lower than the band gap, the difference in energy being supplied by the electric field. This process may be viewed as photon assisted tunnelling of the electron across an energy barrier. In this case, $E_g - h\nu = eF\Delta x$, where F is the magnitude of the electric field and Δx is the tunnelling distance. The absorption coefficient has been derived for the case of transitions $h\nu < E_g$ and is [36,37],

$$\alpha(h\nu) = \frac{2e^2p^2\mu F}{4\pi m^2\hbar^2 n\epsilon c\omega(Eg-h\nu)} \exp[-(E_g-h\nu)/E_0]^{3/2}, \qquad (2.5)$$

where F is the field magnitude, ϵ is the dielectric constant, $\hbar\omega = h\nu$ is the photon energy, μ is the reduced electron-hole mass, p is the momentum matrix element, and E_0 is given by $E_0^{3/2} = 3\hbar F/4(2\mu)^{1/2}$.

The Franz-Keldysh effect has been observed in many crystalline semiconductors, and the above formula is representative of the absorption measured. The hypothesis for amorphous and possibly liquid

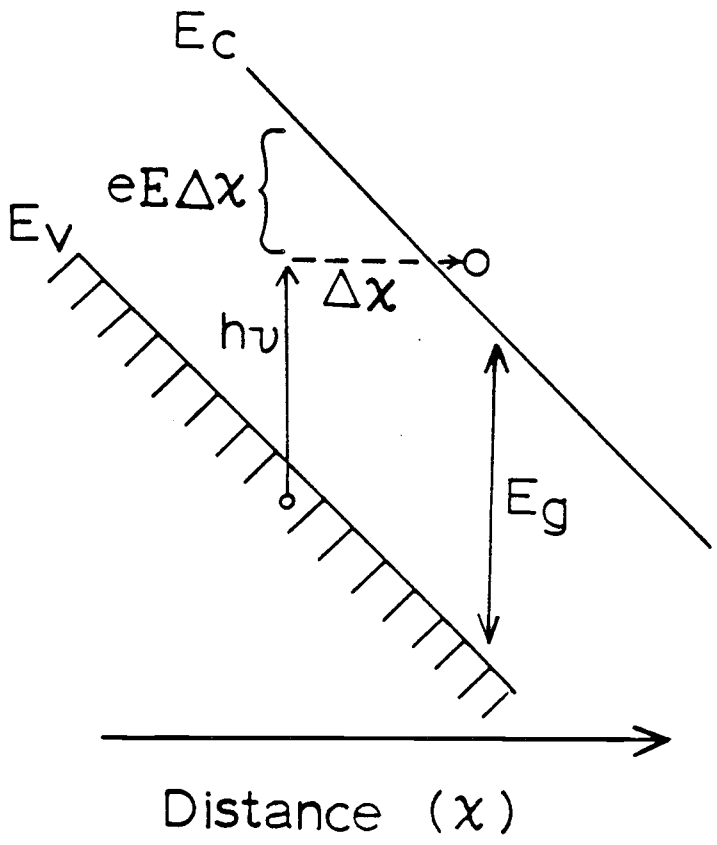

Figure 2.6 The Franz-Keldysh effect.

semiconductors is that disorder and bonding defects lead to a distribution of strong electric microfields within the material, and if absorption occurs on atoms immersed in these fields, a shift of the absorption edge similar to the Franz-Keldysh shift will result. As can be seen from this formula, however, the energy dependence of the absorption is $\exp[(E_g-h\nu)^{3/2}]$, rather than $\exp[(E_g-h\nu)]$, but this may not be an inaccurate result over the limited range of photon energies for some experiments.

There is an immediate question to be considered in this model. Is there indeed a distribution of microfields strong enough to produce a measurable result in an amorphous or liquid semiconductor? A similar question has been examined by Redfield [40,41]. Redfield has averaged the Franz-Keldysh result over distributions of microfields due to impurities in crystalline semiconductors, and has obtained good results. The question as to whether there exist distributions of strong electric microfields within an amorphous or liquid semiconductor has not been satisfactorily answered, and this shall be considered in Chapter 5.

2.3.4 Excitonic effects

In addition to the electric field shift of the absorption edge, there exists the possibility that excitonic effects may be important in an amorphous or liquid semiconductor. By excitonic effects, it is not implied that bound excitonic states exist, such as occur in crystals at low temperatures, but rather an appreciable interaction between the

excited electron and the hole it leaves behind in the valence band. If such an interaction exists, what is its effect on the optical absorption edge? This question has been examined in detail by Dow and Redfield [42,43,45] and by Dow and Hopfield [44]. They considered the change in the Franz-Keldysh effect concomitant with an electrostatic interaction between the electron and hole. The basic idea is this: The interaction between the electron and hole is, in the center of mass system $V_i=-e^2/\epsilon r$. The potential due to the local electric field is $V_z=-eFz$. When the interaction V_i is appreciable, in addition to the potential drop across the exciton radius, then excitonic effects are significant and must be taken into account.

The absorption coefficient for a uniform field and with excitonic effects included has been derived by Dow and Redfield [42,43]. Their derivation is based on the Elliot theory of optical absorption by excitons [46]. In the Elliot theory, the absorption for allowed transitions ($\mathbf{k} \rightarrow \mathbf{k}$) is proportional to the probability density of the exciton wave function at $\mathbf{k}=\mathbf{0}$ [58]. For energies less than the band gap, the absorption coefficient in the Dow-Redfield model is:

$$\alpha(h\nu) = \frac{8\pi^2 e^2 p^2}{m^2 n c \omega R a^3} \cdot |U(h\nu)|^2, \qquad (2.6)$$

where R is the Rydberg energy $R=e^2/2\epsilon a$, and a is the modified Bohr radius, $a=\epsilon a_0$. The quantity $|U(h\nu)|^2$, which is related to the probability density of the electron-hole wave function at zero wave vector, must be derived numerically. Dow and Redfield evaluated this quantity over nine orders of magnitude and found it to be nearly exponential at all energies where it was evaluated. They argued on that basis the common origin of the Urbach rule in ionic and covalent solids. Although their interest was in the Urbach rule in solids, the same model can be used as a basis for the interpretation of the exponential absorption in liquids. We will call this model the "ionic model."

2.3.5 The ionic model

A different way to view the shift of α with temperature (on a plot of α vs. $h\nu$) is to consider that the shift is vertical, rather than horizontal. In other words, the absorption is, *for a given energy*, increasing with temperature (or in alloys, with metallic component concentration). This viewpoint does not require a shift of the band gap. It does, however, require a mechanism which enhances the absorption as the temperature or concentration of metallic component increases. Such a mechanism can be realized in a combination of the Dow-Redfield model and a microfield distribution given by the distribution of fields surrounding ionic atoms in the liquid. The absorption can be calculated in this model by assuming that the absorption per atom is that given by the Dow-Redfield result. This absorption can then be averaged over a

distribution of microfields that is, apart from normalization, just the volume per field increment, dV/dF, surrounding an ion. dV/dF can be calculated from electrostatics. The overall absorption is then proportional to the concentration of ions, which increases with temperature by thermal activation. The ionic model is central to this thesis, and one of the goals of this work is to establish that it can give a satisfactory explanation for optical absorption in liquid semiconductors where ions are present. In Chapter 5, a detailed description of this model is given, the absorption expected from it is calculated, and it will be demonstrated that it gives results in good agreement with the data.

2.4 Motivation for the present study

In order to differentiate between the above mentioned models, it is necessary to examine the dependence of the measured absorption on those factors which can be changed experimentally. These factors are: the temperature, the photon energy, and in the case of an alloy, the concentration. The motivation for this study was to carefully measure the dependence of α on each of these factors in order to determine whether the band gap would shift and if one could expect a significant density of gap states or internal electric microfields. Finally, there was the motivation to determine whether the magnitude and shape of the absorption as calculated in the Franz-Keldysh and Dow and Redfield models would be consistent with the observed absorption.

3. EXPERIMENTAL ARRANGEMENT

3.1 The optical cell

Measurements on the Se-Tl liquid alloy system were made using an optical absorption cell of an original design developed in our laboratory. A complete description of the cell has been given elsewhere [48], and only a brief description will be given here. The basic requirements are to construct a high temperature optical cell which is transparent over the visible range and into the near infrared. It must also be reusable, inert to the sample, and of variable thickness.

The working design is shown in Figure 3.1, and is a combination of an optical cell and filling reservoir. The cell essentially consists of a sandwich of two plane parallel optical windows (inert to the semiconductor at high temperatures) and a gasket made of Grafoil [49] which seals the cell and defines the optical aperture. The gasket also defines the cell thickness. A narrow channel cut vertically in the Grafoil allows the cell to be filled with the liquid sample. The cell was filled by evacuation and subsequent injection of the fluid using inert gas at one atmosphere pressure.

Cells of variable thickness were constructed by: (1) using Grafoil gaskets of thicknesses 127, 254, and 381 μm; (2) relieving one surface of one optical window to decrease the cell thickness; or (3) inserting a ceramic spacer to increase the thickness. Cells of three different thicknesses, 3400 μm, 381 μm, and 54 μm were used throughout the

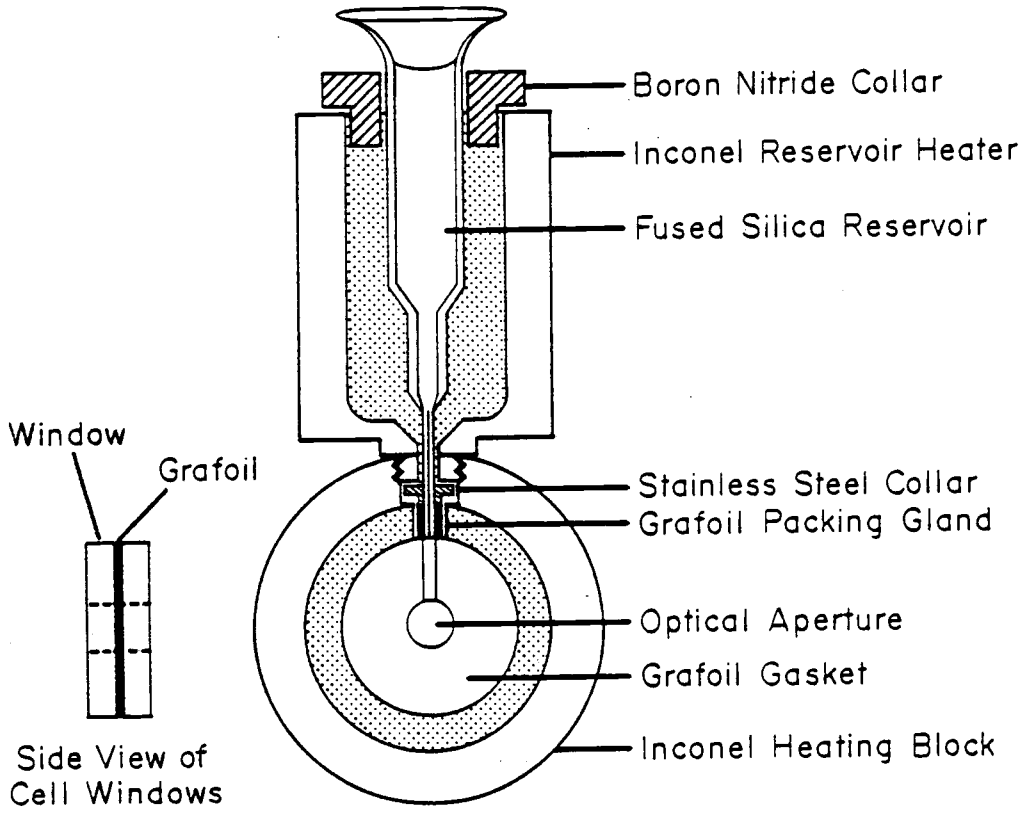

Figure 3.1 The optical cell and reservoir. Inset shows side view of cell sandwich.

study to provide overlap in the measurement of absorption for different runs. Sapphire windows were used for all measurements.

The maximum absorption which could be measured with this cell was limited by stray light, and was around $\alpha d \approx 7$, where α is the absorption coefficient and d is the cell thickness. Alignment errors limited the minimum measureable absorption to about $\alpha d \approx .05$. Maximum attainable temperature with this cell was around 550 °C, but most measurements were confined to temperatures less than 475 °C for safety reasons. For a detailed description of the experimental limitations, see Ref. 48.

A variation of the optical cell appropriate for measurements of extended X-ray absorption fine structure (EXAFS) in liquid semiconductors has been constructed by this author. This cell is described further in the Appendix.

3.2 The optical arrangement

The experimental layout is shown in Figure 3.2. The source was a tungsten halogen projector lamp, and the monochromator a Jarrell-Ash Mark X modified to accept six gratings to cover the entire spectral region. The signal detector was a liquid-nitrogen-cooled HgCdTe narrow-gap-semiconductor detector. The experiment was controlled and data was obtained automatically with an Apple IIe™ microcomputer.

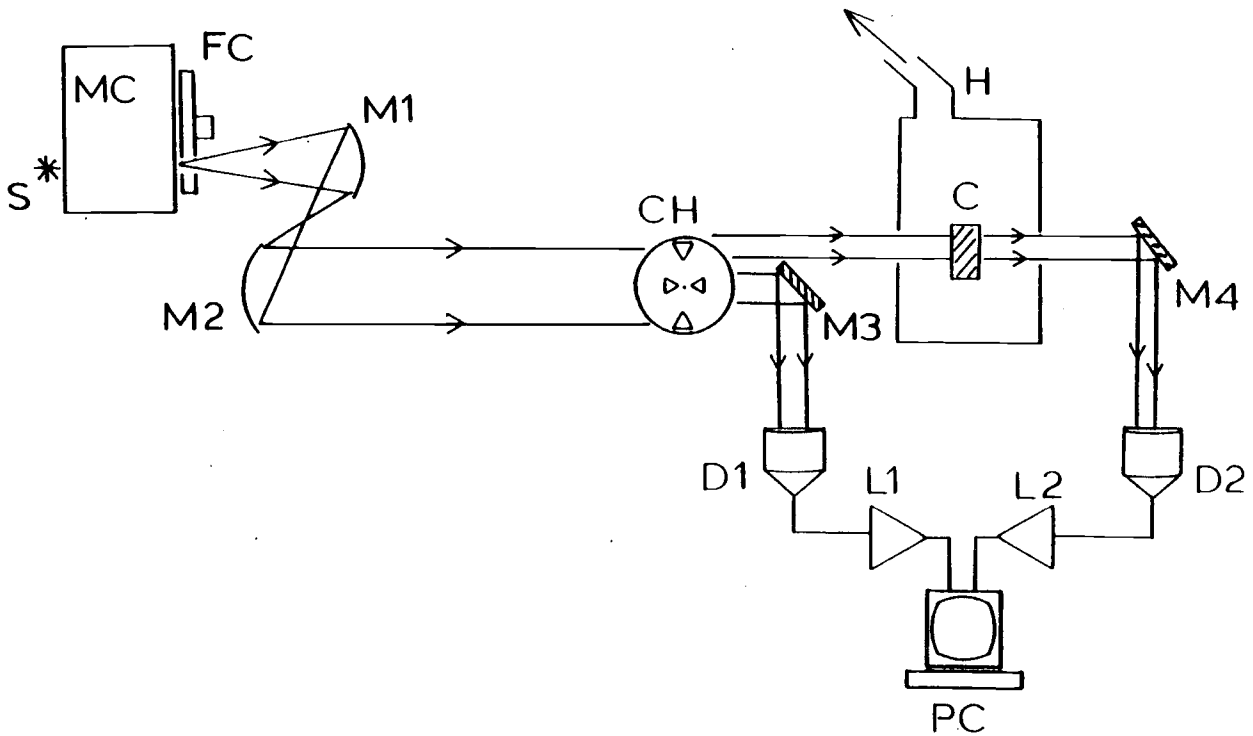

Figure 3.2 Optical layout. C: cell; CH: chopper; D1, D2: detectors;FC: IR filter carousel; H: fume hood; L1, L2: lock-in amplifiers; M1, M2: collimation mirrors; M3, M4: focussing mirrors; MC: monochromator; PC: Apple IIe™ computer; S: tungsten halogen source.

Absolute absorption measurements were obtained by splitting the light beam into two beams, and recording the ratio of the light transmitted through the cell to light detected at a reference detector. This eliminated effects of fluctuations in source intensity over time. Calibration of the intensities was accomplished by measuring the transmittance through the filled cell and comparing this to the transmittance through the empty cell, which had been previously recorded and stored on computer. Reproducibility in the calibration determined the overall uncertainty in the measurements, and was about 5%. Reflectivity corrections were not made to the data, for reflectivity losses at the measurement wavelengths were less than the uncertainty in calibration. Further details of the method of measurement and apparatus are described in Ref. 48. Also described therein are the sources of error and their effect on the accuracy of the data.

3.3 Sample preparation

Individual samples were made using the following technique: First master alloys were prepared by grinding 999.99% purity selenium in a mortar and adding thallium to obtain concentrations of 10%, 5%, and 1% atomic fractions. The thallium had been previously soaked in spectroscopically pure methanol to remove oxides. These mixtures were placed in sealed, evacuated (100μm vacuum) fused silica tubes and brought to 500°C in a crucible furnace. The tubes were held at this temperature for 5 hours and rotated periodically while hot and in a nearly horizontal

position to insure mixing. At the end of the mixing period, the tubes were thrust quickly into water at room temperature and solidification occurred within ten to fifteen seconds. The quartz tubes did not break upon the quenching.

After quenching, the quartz enclosures were dried, then broken and the materials removed. These master alloys were then ground in a mortar to a fine powder and kept in sealed containers, and they became the dopants used to prepare the experimental alloys. The experimental alloys were prepared in exactly the same way, by mixing proportional amounts of selenium powder and dopant powder, mixing at high temperature, and quenching in water. After removal of the experimental alloys from the quartz tubes, they were broken into small pieces, and the entire sample was placed in the reservoir of the cell. The reservoir was then flushed with inert gas and an inert gas atmosphere was maintained during the experiment.

3.4 Concentration uncertainty

It turns out that the major uncertainty in the experiment was not that inherent in the measurements themselves, but that of concentration. It was hoped that by only preparing the samples directly before measurement (within one day) and by using the entire sample in a given experiment, errors in concentration could be kept to a minimum. However, it was found that for some of the concentrations, there must have resulted uncertainties of the order 5-10% in the concentration. This could be

seen from observation of the scatter for some concentrations in a plot of absorption vs. concentration, at given photon energies and temperatures (see next chapter). Uncertainty of this amount is difficult to explain, for even though measurements for some of the concentrations were repeated after extreme care in preparation of the samples, reproducibility within a few per cent was not always possible.

A possible source of uncertainty in the concentration is due to evaporation of the sample. Evaporation results because the cell does not have a hermetic seal, and this is a basic limitation of the cell design. This limitation arises in two ways. As mentioned earlier, the cell is filled by applying a moderate vacuum (100 μm), and then forcing the fluid into the cell aperture under pressure. It is expected that Se, which has a higher vapor pressure than Tl, would distill upon the application of vacuum, thereby increasing the Tl concentration. This effect would be more significant at the largest Tl concentrations. The measured absorption was noticed to increase after repeated emptying and refilling, indicating that the Tl concentration had, in fact, increased, and repeated fillings of the cell were avoided for this reason.

The evaporation problem also limits the range of measurement to temperatures below the boiling point of the sample at atmospheric pressure. In the experiment, it was found that a considerable vapor leak occurred above 550 °C, and for this reason, no measurements were made above this temperature, and Se was the only sample for which measurements were made above 475 °C.

Another possible source of error in the concentrations may be due to the presence of oxygen in the original selenium. There is evidence that oxygen is present in the pure selenium at concentrations of the order .08 mass per cent [57]. We expect that this oxygen would be entirely purged by the addition of thallium metal with the reaction:

$$2Tl + 3O \rightarrow Tl_2O_3. \qquad (3.1)$$

This has the effect of removing Tl and reducing the concentration below the nominal value in the master alloys. Therefore the experimental alloys made from the master alloys would be reduced in Tl concentration a corresponding amount. In Table 3.1 we list the nominal concentrations and the corrected concentrations expected after removal of oxygen. The concentrations x=.001, .002, and .003 are nominal, i.e., these concentrations are calculated to be x=.00113, .00214, and .00312, respectively, as prepared.

Table 3.1 Concentrations expected for the complete removal of oxygen from selenium by the addition of thallium. Concentrations are in atomic per cent thallium.

Nominal Conc.	Calculated Conc.	Corrected Conc.	% Diff.
Experimental alloys:			
.001	.00113	.00110	2.7
.002	.00214	.00205	4.2
.003	.00312	.00307	1.6
.005	.005	.00491	1.8
.007	.007	.00688	1.7
.009	.009	.00884	1.8
Master Alloys:			
.010	.010	.00982	1.8
.050	.050	.0477	4.6
.100	.100	.0979	2.3

As can be seen from these results, uncertainties of the order 5-10% can not be accounted for by the presence of oxygen.

3.5 Summary

An infrared absorption cell has been designed which can be used for absorption studies of liquid semiconductors at high temperatures. Because the cell is assembled using a clamping technique with a gasket, the optical windows can be of any optical material chemically compatible with the sample. This has eliminated the need for fused quartz cells, and removes the infrared cutoff limit of cells used in the past. The cell can easily be constructed to have any thickness between 50μm and .5 cm, allowing the measurement of absorptions from 2×10^{3} to .1 cm^{-1}.

There are two limitations of the cell design. The first is the minimum thickness, which is limited by the tolerance with which the offset windows can be ground by conventional machining techniques. The second is that the cell does not have a hermetic seal. This limitation prevents measurement of absorption for temperatures above the boiling point of the sample. It also can cause changes in the concentration of alloys which have high vapor pressures.

A cell of similar design using boron nitride windows in place of the optical windows has been successfully used for EXAFS measurements on liquid Se and Se-Te alloys up to 450 °C.

4. DATA PRESENTATION AND ANALYSIS

4.1 Raw data

The absorption coefficient, α, in liquid $Se_{1-x}Tl_x$ alloys has been measured for x = 0, .001, .002, .003, .005, .007, .009. The results are shown in Figures 4.1-4.12, where $\ln \alpha (cm^{-1})$ is shown as a function of photon energy, $h\nu$ (eV). Each figure corresponds to an individual concentration, the concentrations x=.001, .002, and .003 being nominal. These concentrations are x=.00113, .00214, and .00312, respectively. The absorption as a function of $h\nu$ is essentially exponential over the range of photon energies measured, and the absorption increases with temperature and Tl concentration. These observations are qualified below.

4.1.1 Low temperature effect

It will be noticed in some of the alloys that there is a deviation from the exponential behavior at low temperatures, and low absorption values. This is seen as a bend or levelling of the curves toward constant absorption as the energy decreases. This behavior can be explained on the basis of immiscibility in Se-Tl liquid alloys. It is known that a region of liquid immiscibility exists which is centered at about 10 atomic per cent Tl at low temperature, as can be seen from the phase diagram in Figure 4.13 [50]. In this region, a second, Tl-rich phase of composition ~ $Se_{.8}Tl_{.2}$ separates at a low enough temperature which

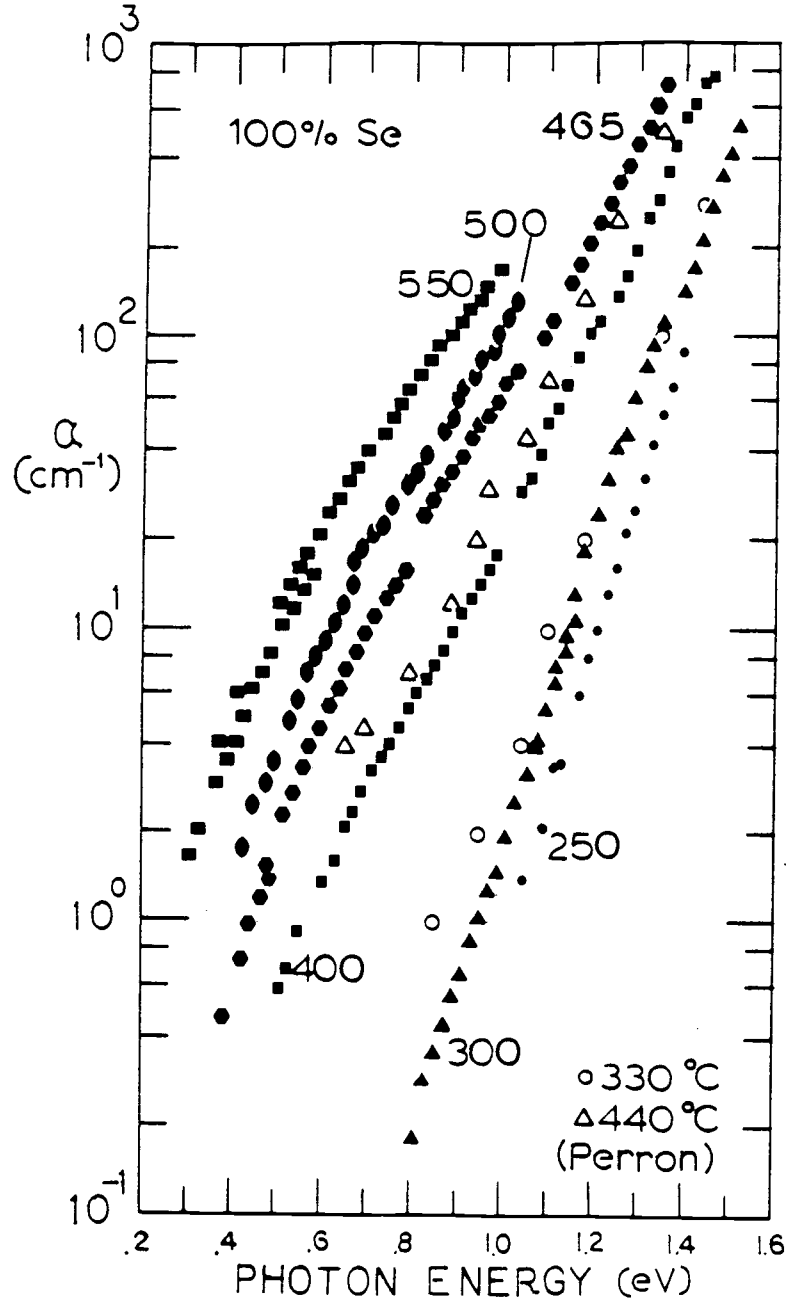

Figure 4.1 Absorption in liquid selenium. Closed symbols are this work, open symbols are from Perron, Ref. 1 and 16.

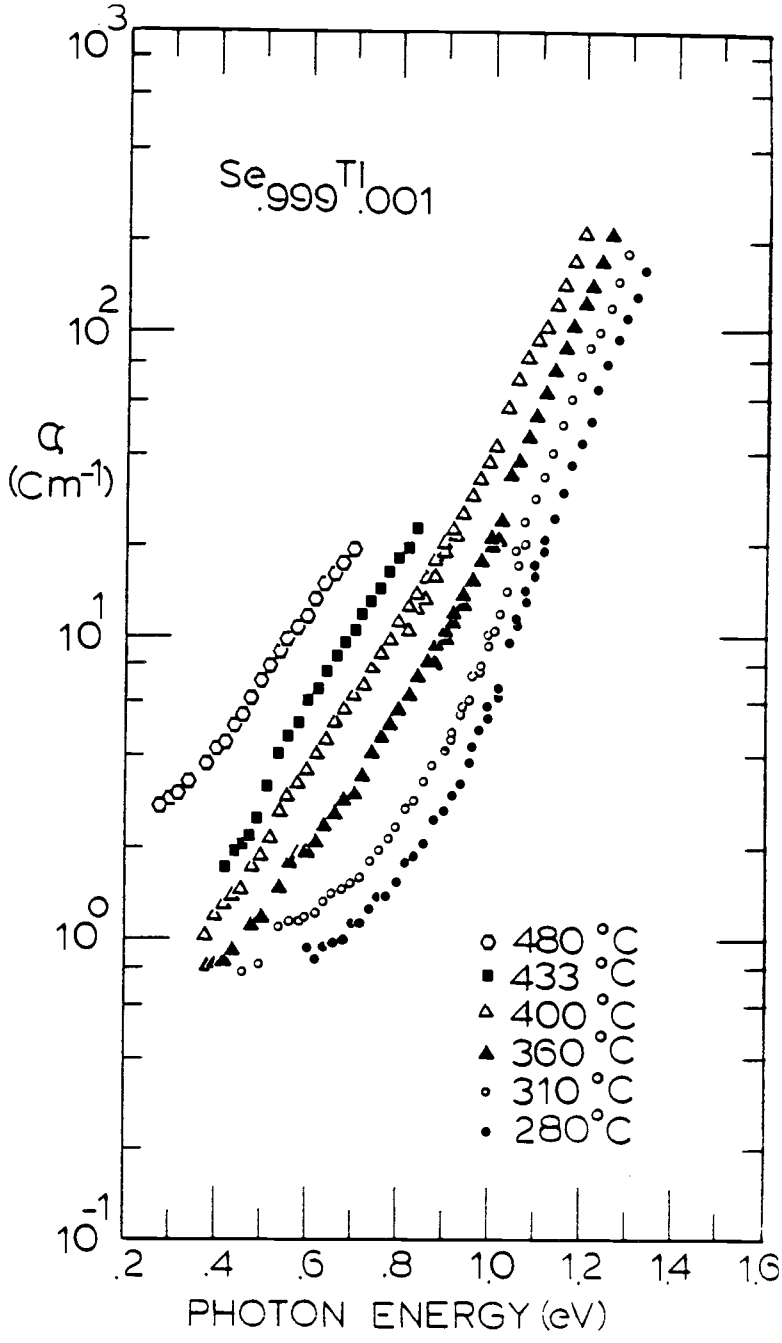

Figure 4.2 Absorption in $Se_{.999}Tl_{.001}$.

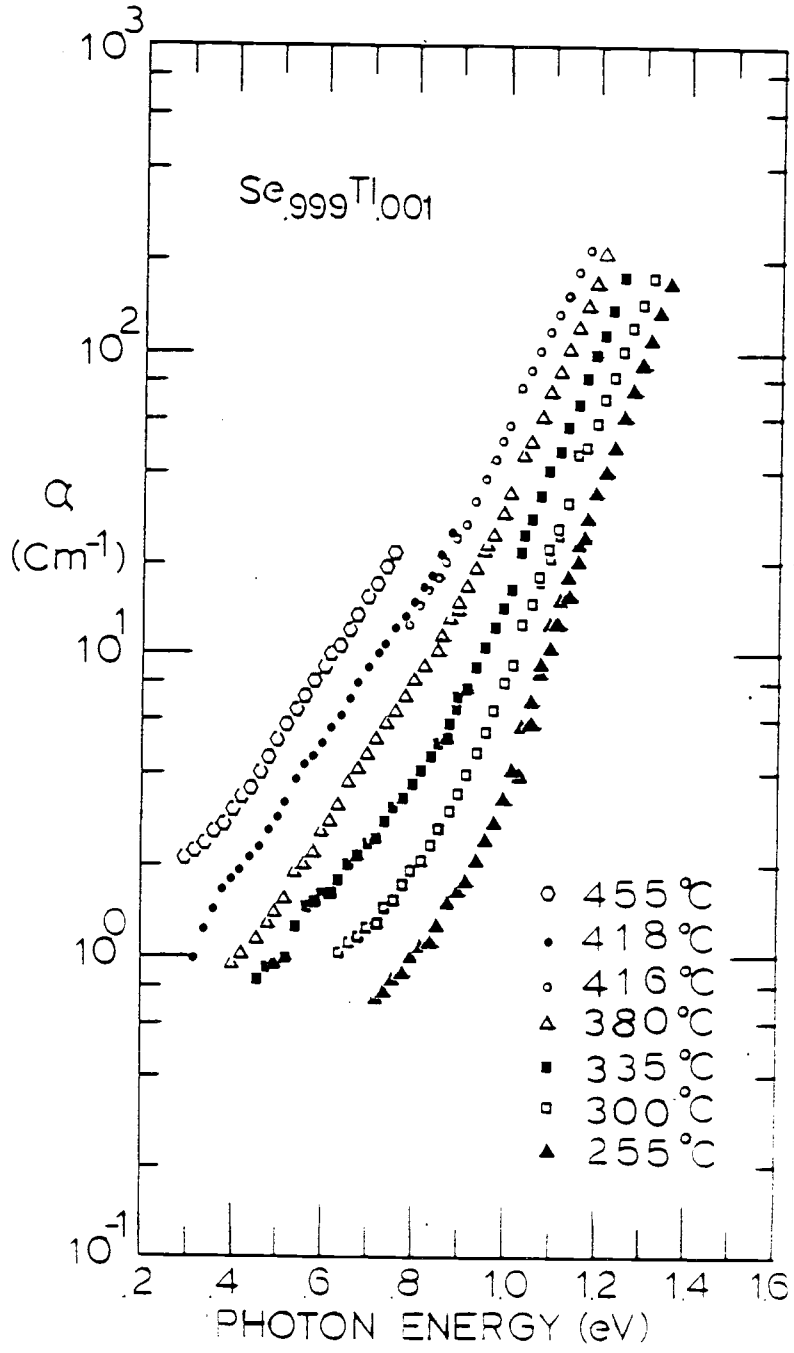

Figure 4.3 Absorption in $Se_{.999}Tl_{.001}$.

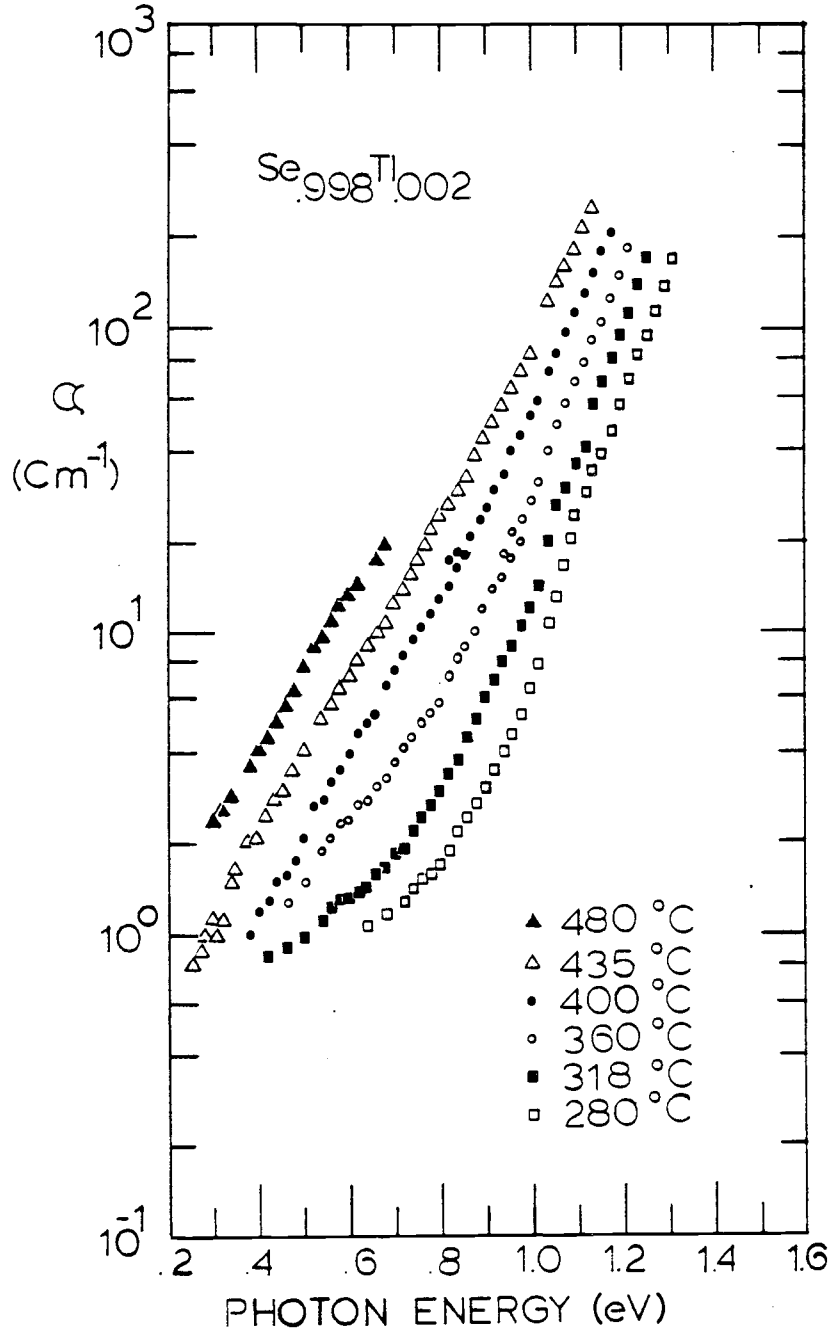

Figure 4.4 Absorption in $Se_{.998}Tl_{.002}$.

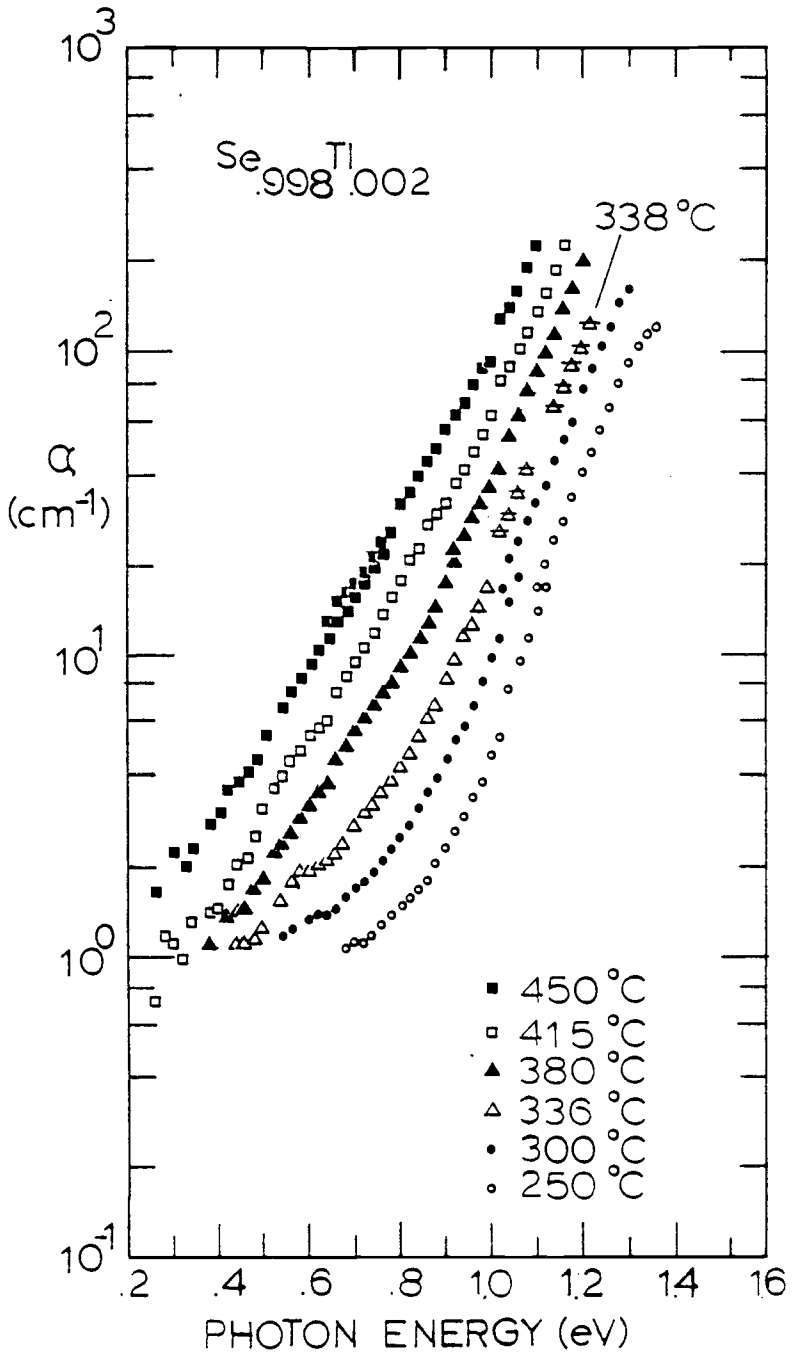

Figure 4.5 Absorption in $Se_{.998}Tl_{.002}$.

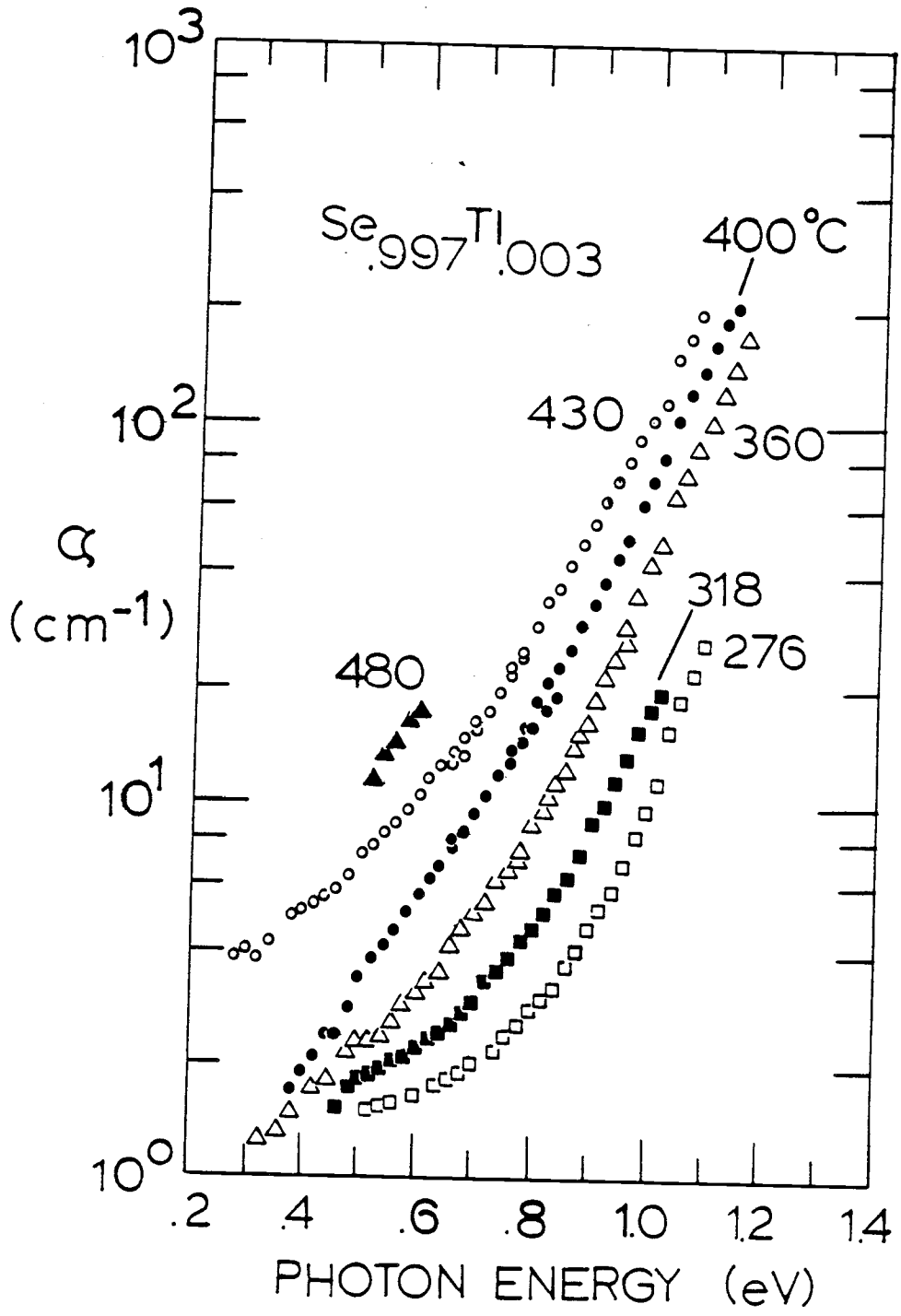

Figure 4.6 Absorption in $Se_{.997}Tl_{.003}$.

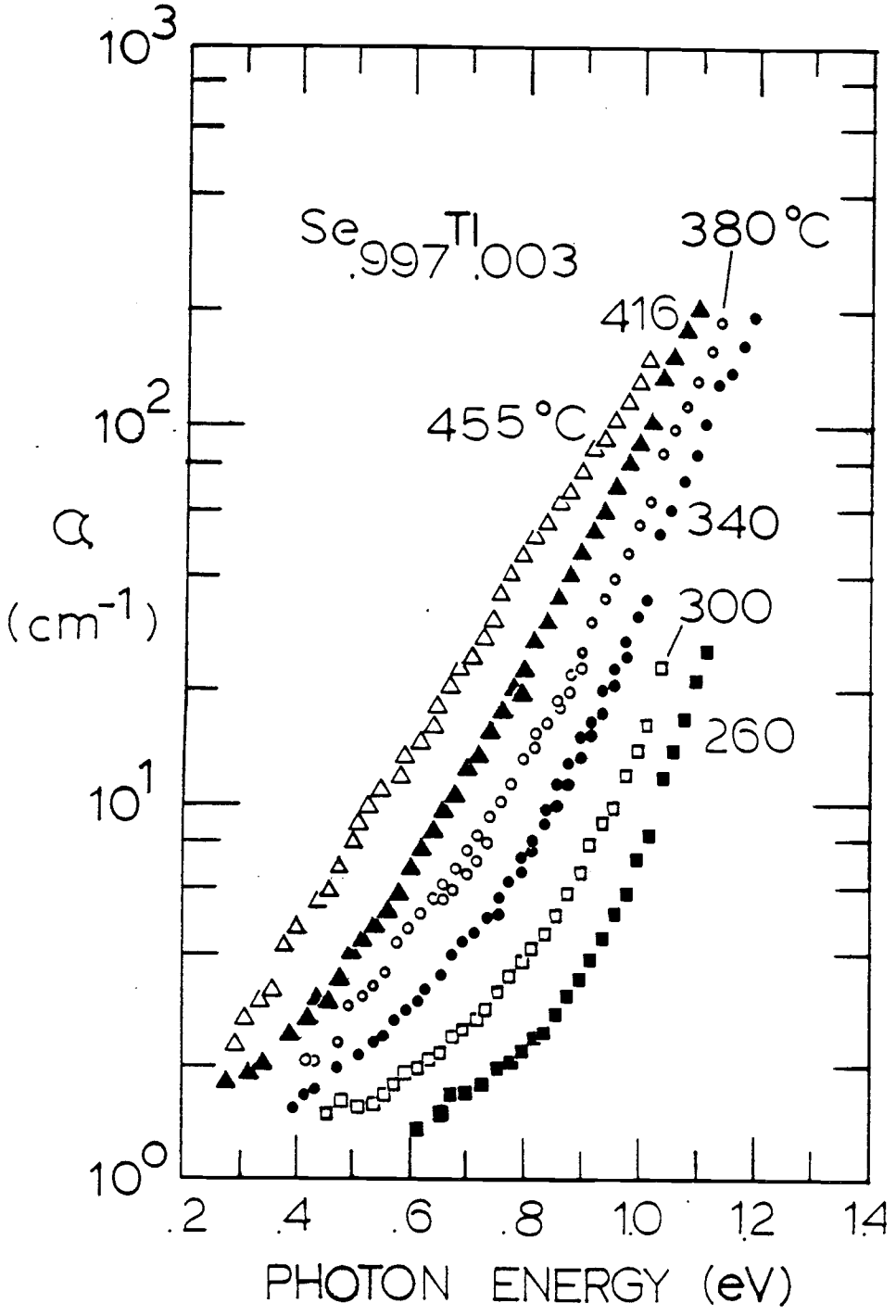

Figure 4.7 Absorption in $Se_{.997}Tl_{.003}$.

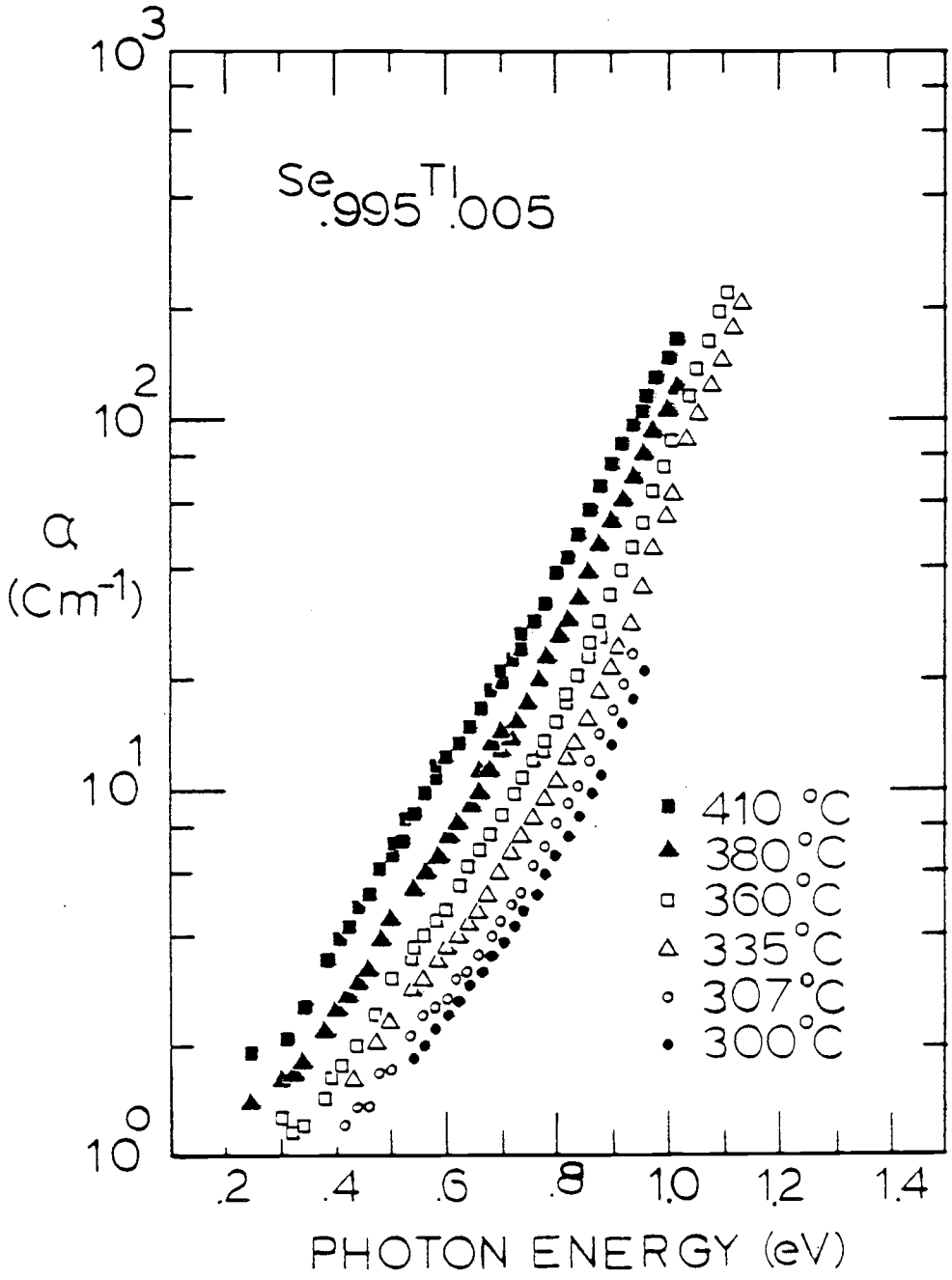

Figure 4.8 Absorption in $Se_{.995}Tl_{.005}$.

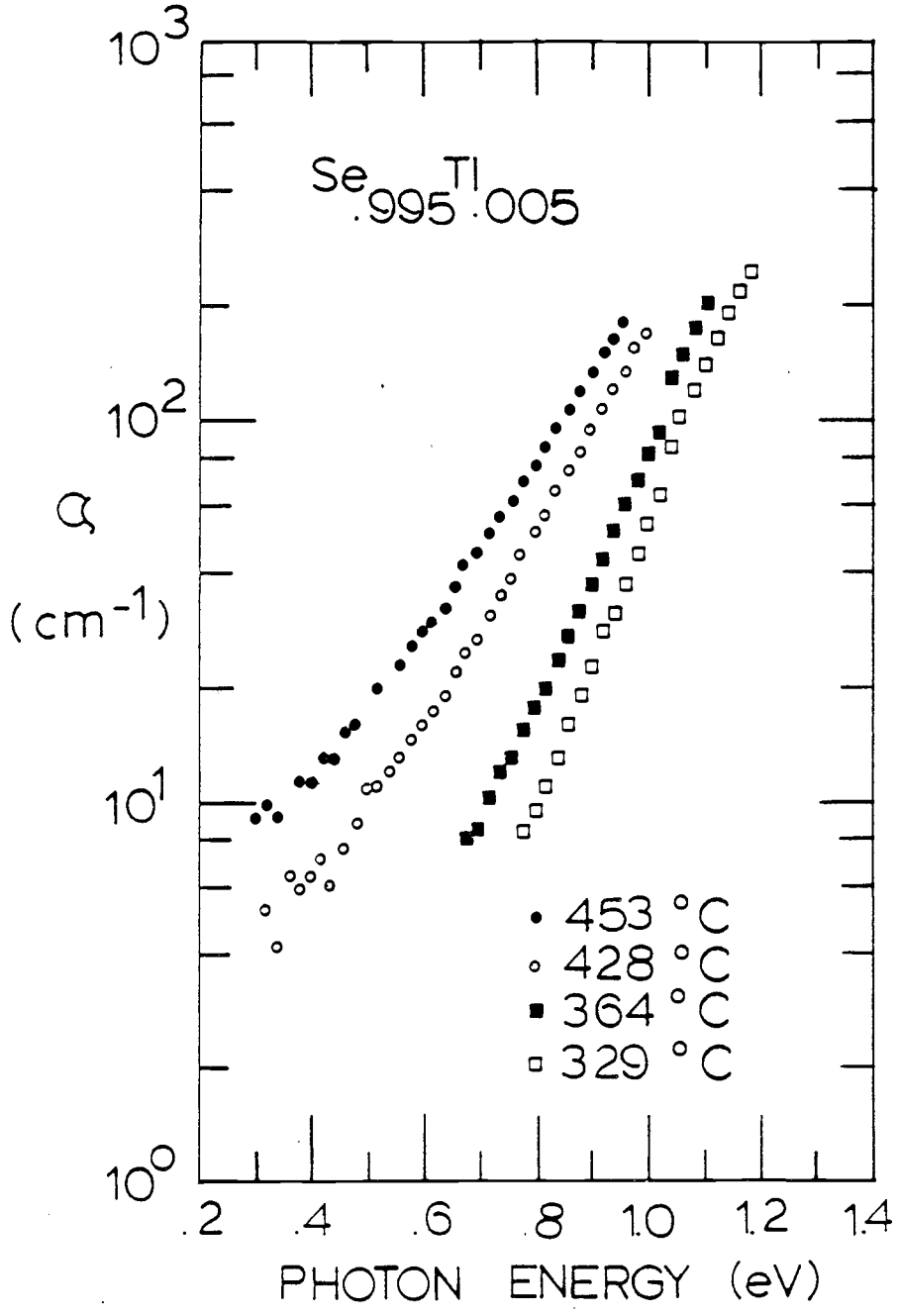

Figure 4.9 Absorption in $Se_{.995}Tl_{.005}$.

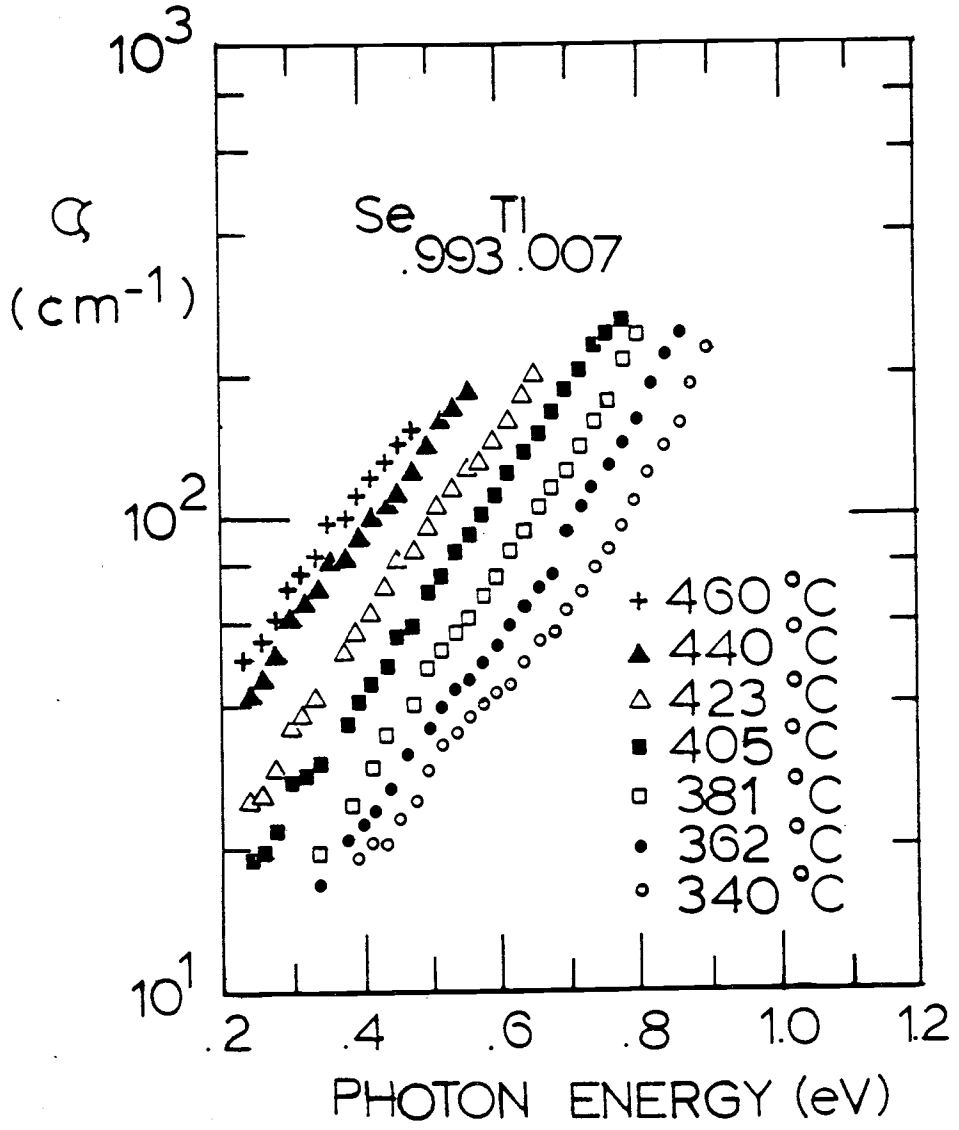

Figure 4.10 Absorption in $Se_{.993}Tl_{.007}$.

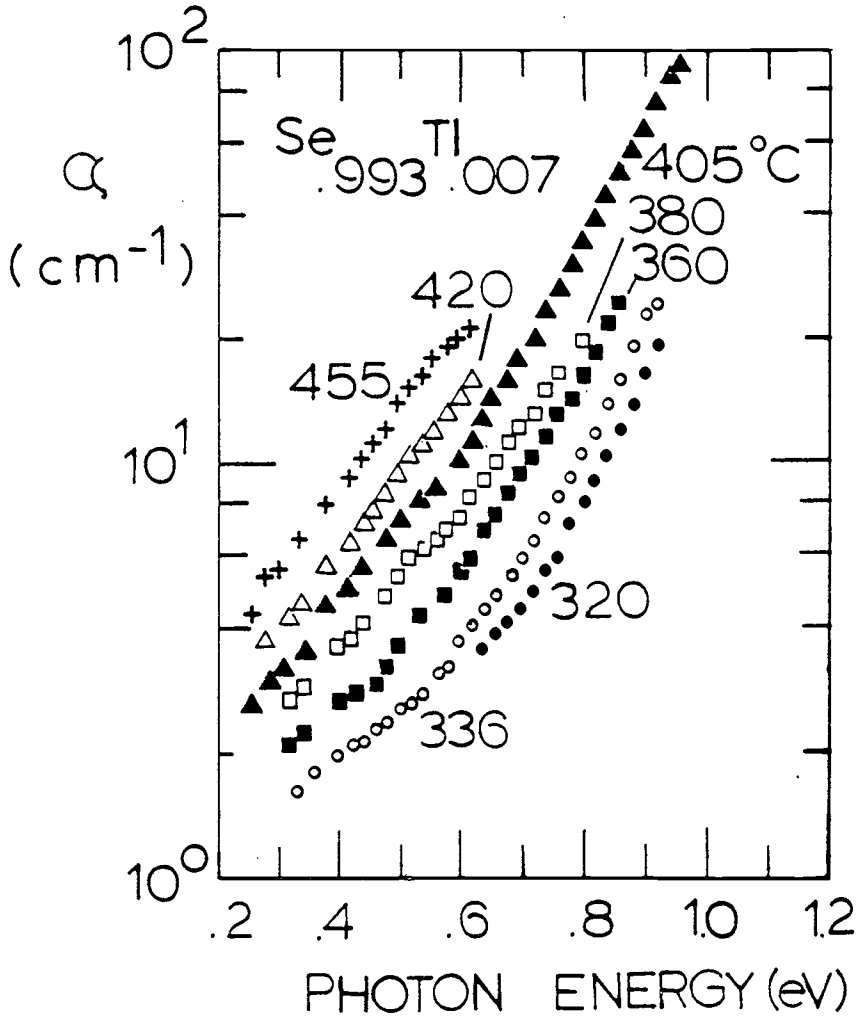

Figure 4.11 Absorption in $Se_{.993}Tl_{.007}$.

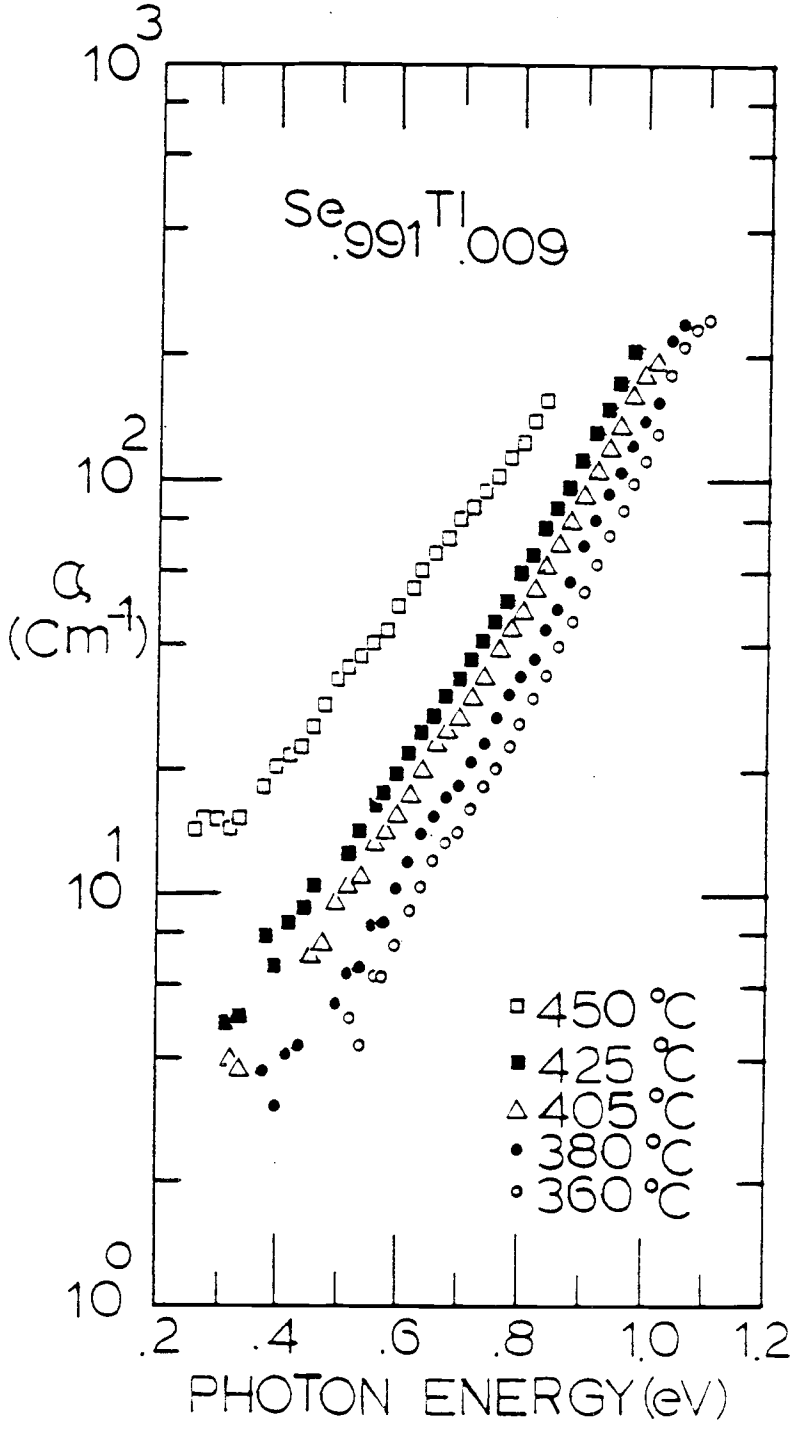

Figure 4.12 Absorption in $Se_{.991}Tl_{.009}$.

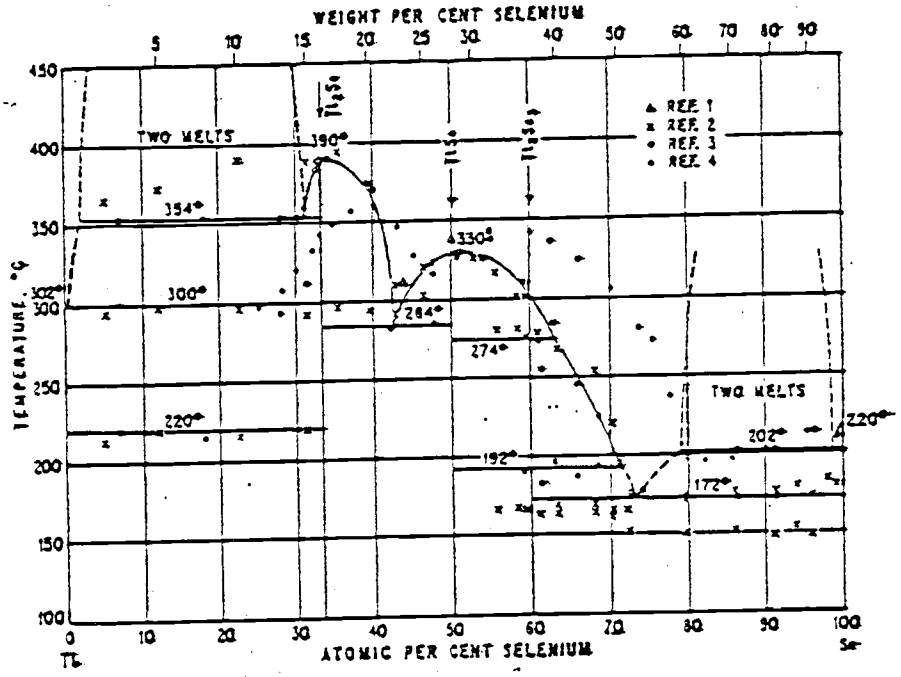

Figure 4.13 Phase diagram for Se-Tl.
From Ref. 50.

depends on x. The present work is confined to the region for $1-x > .99$. Petit and Camp [51] have measured conductivity in this and other regions and provide more detailed information for the temperatures at which two liquids occur. In the present study, it was simple to define the temperature at which immiscibility occurred for a particular concentration, by measuring the absorption at a particular photon energy as the temperature was lowered. It was observed that the absorption decreased continuously, then increased abruptly at a particular temperature. It is believed that at this temperature, small droplets of a second liquid form which are high in Tl concentration and are of the order one micron in diameter. The viscosity of the solvent prevents these droplets from falling out of suspension. The light which passes through the sample scatters from these small droplets, and is lost from the beam. This is realized as an increase in absorption as measured from the transmitted intensity.

By measuring the temperature at which the absorption increase occurred in several concentrations for a particular photon energy, this temperature could be predicted for other concentrations. The results of this observation for $h\nu=1$ eV are shown in Figure 4.14, along with the results reported by Petit and Camp. Although the present results indicate higher immiscibility temperatures than those of Petit and Camp, super- cooling of the liquid beyond this temperature cannot be ruled out in either case. Therefore, data must be disregarded for temperatures close to the immiscibility point for a given alloy and the bending of the

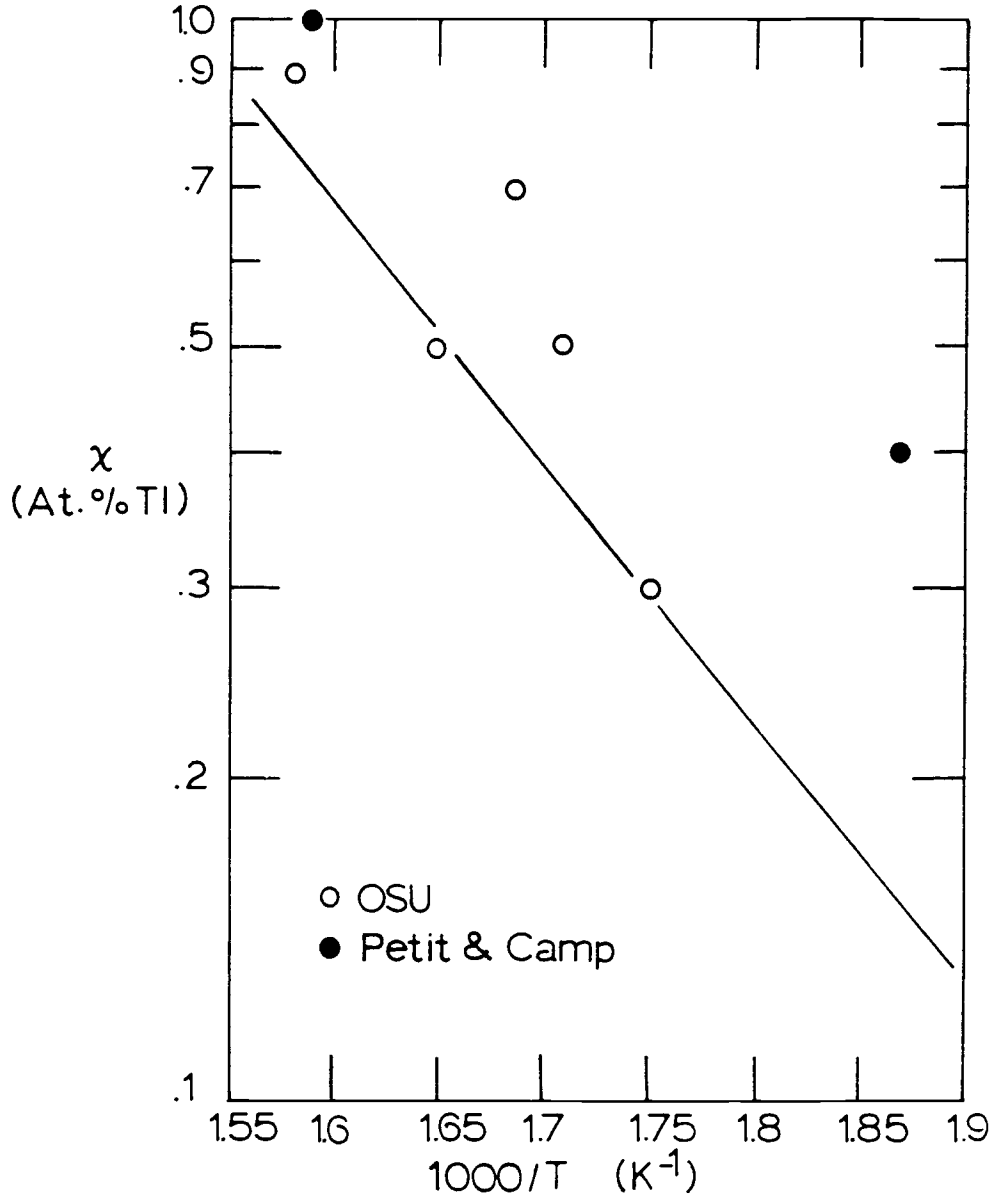

Figure 4.14 Phase separation temperatures for indicated concentrations x (in At. % Tl). Open symbols, this work, closed symbols, from Ref. 51.

ln α vs. $h\nu$ curves at low temperatures should be regarded as suspect. Fortunately, this comprises only a small portion of the total data set.

4.1.2 Extrapolation to the band gap

As mentioned in Chapter 2, the increase in absorption with concentration and temperature might be interpreted as a decrease in the optical band gap. This interpretation can be tested by extrapolating the absorption curves up to an absorption value expected to be representative of the band gap. This value is taken to be $\alpha \approx 10^5$ cm^{-1}. The results of this extrapolation are shown in Table 4.1.

Table 4.1. Extrapolated band gap at $\alpha = 10^5$ cm^{-1} for selected temperatures and concentrations. Energies are in eV.

Temperature	Concentration (At. % Tl)						
(°C)	0	.1	.2	.3	.5	.7	.9
250	1.95	1.99	2.13				
300	1.98	1.97	2.07				
360	1.90	1.98	1.96	1.95	1.85	1.59	1.98
400	2.08	1.99	1.94	2.01	2.26	2.08	2.03
415		2.00	2.01	1.97	2.10		
450	2.03	2.20	2.10	2.22	2.21		2.25

The values of the band gap obtained this way give an average E_g=2.0±.1, with no observable trend as a function of concentration or temperature. This result is in disagreement with the interpretation of the absorption increase as a decrease of the band gap.

4.2 Concentration dependence

The dependence of absorption on concentration can be seen from a plot of α vs. x for a particular energy and temperature. Representative plots for 340 °C and 400 °C are shown in Figures 4.15 and 4.16. The absorption coefficient was found to increase linearly with concentration for all temperatures and energies. There is some deviation in this rule for some concentrations, which we believe to be due to errors in the concentration, as discussed earlier. Uncertainties notwithstanding, we may write generally,

$$\alpha(h\nu,x)_T = \alpha_1(h\nu) + x\cdot\alpha_2(h\nu) \; . \qquad (4.1)$$

It can be seen from Figures 4.15 and 4.16 that the intercept at x=0 (i.e. α_1) is non-zero. This quantity can be compared to the absorption in 100% Se at respective temperatures and energies. This is illustrated in Figure 4.17 for 400 °C, where the absorption measured in pure Se is plotted vs. $h\nu$ along with the intercept, α_1, as calculated using a least squares fit to

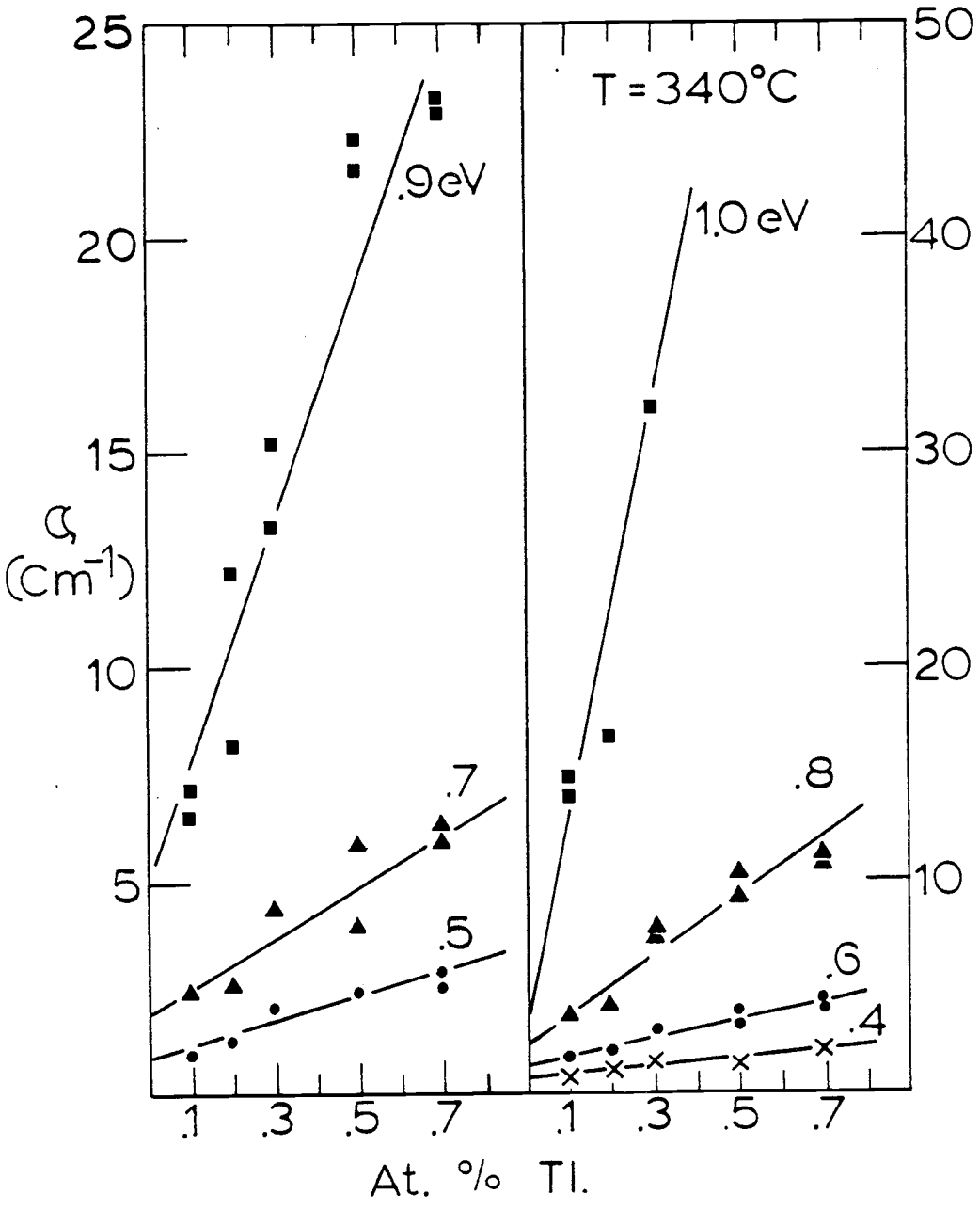

Figure 4.15 Absorption coefficient vs. thallium concentration at 340 °C, for selected energies. Left ordinate is for left half of plot, right ordinate, for right half.

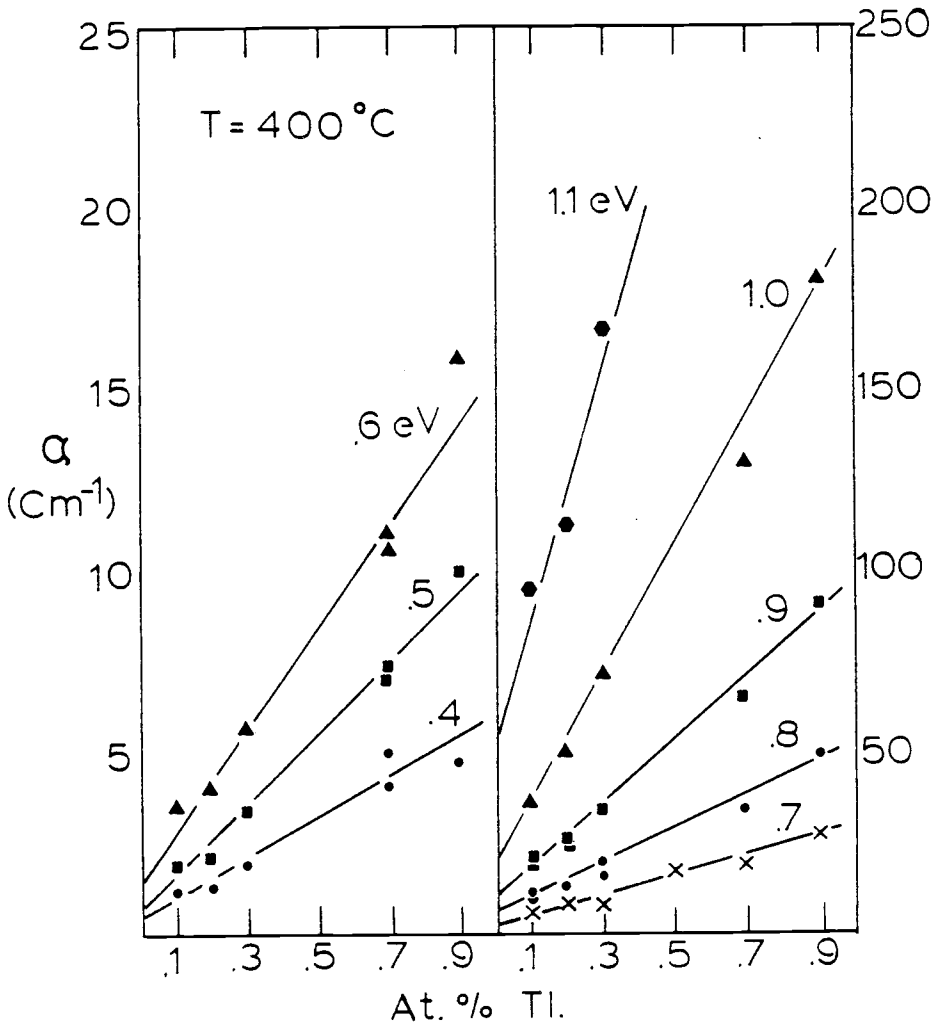

Figure 4.16 Absorption coefficient vs. thallium concentration at 400 °C, for selected energies. Left ordinate is for left half of plot, right ordinate, for right half.

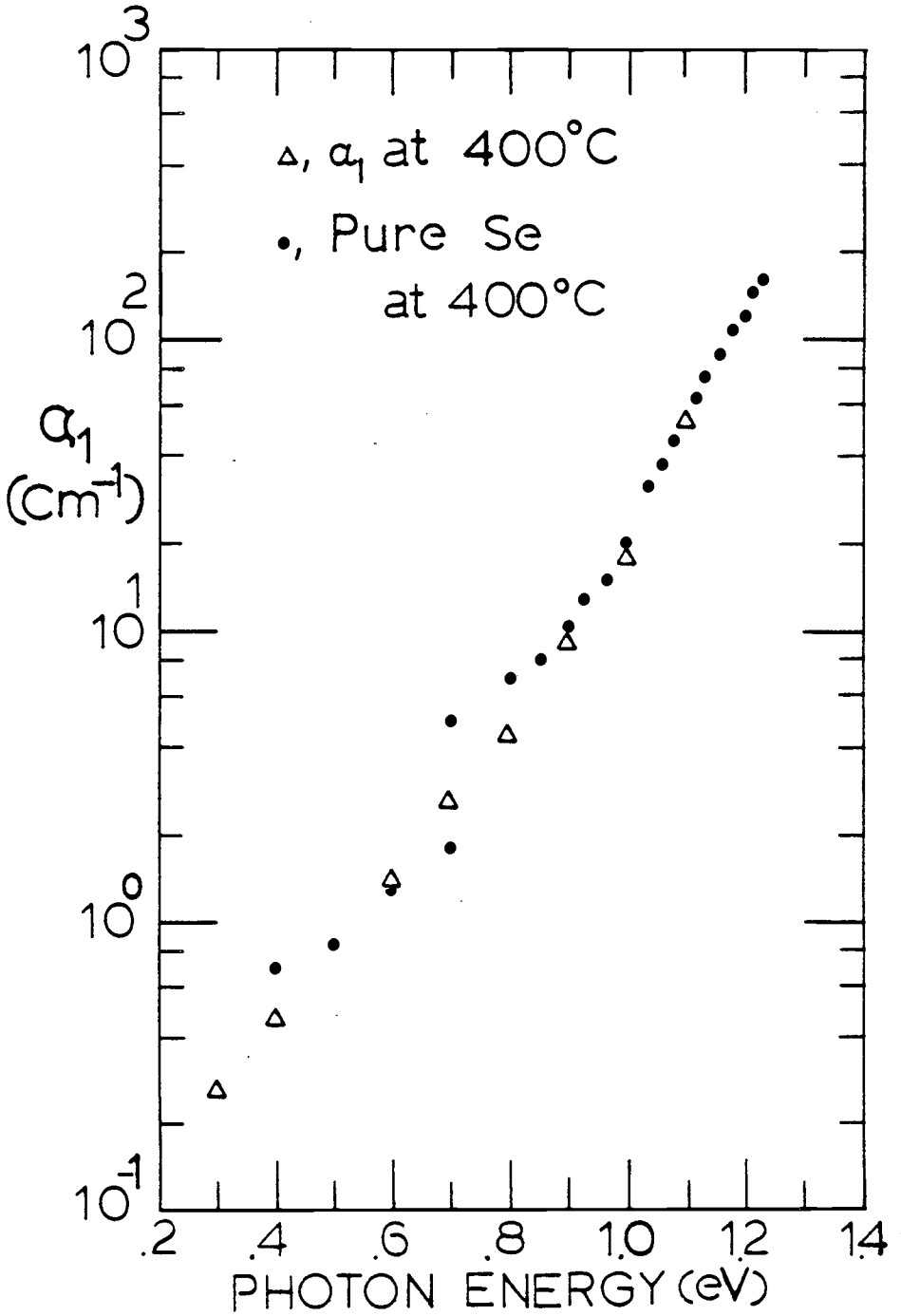

Figure 4.17 α_1 and α_{Se} vs. photon energy at 400 °C

α_T vs. x. Although the correspondence is good at this temperature, uncertainties in the evaluation of α_1 are significant. Therefore we may regard the dependence of α vs. x to be linear, and the intercept may be identified with that absorption present in the absence of Tl, but any analysis involving either α_1 or $\partial\alpha/\partial x$ would be moot. For completeness, the parameters α_1 (upper listing) and $\partial\alpha/\partial x = \alpha_2$ (lower listing) are given in Table 4.2 for several selected temperatures and photon energies as obtained from a linear least squares fit to α_T vs. x.

Table 4.2. Parameters from linear least squares fit of α vs. x.
Upper value, intercept (cm^{-1}); lower value, slope (cm^{-1}).

Photon Energies (eV)	Temperatures (°C)					
	340	360	380	400	420	450
0.4	.69	.60	.56	.47	.53	
	.18	.27	.37	.53	.74	
0.5	.84	.86	1.0	.41	.72	
	.28	.41	.55	1.0	1.3	
0.6	1.3	1.2	2.1	1.4	1.9	1.5
	.39	.67	.92	1.5	1.9	4.8
0.7	1.8	1.1	2.5	2.6	3.5	.77
	.63	1.3	1.7	2.4	3.2	8.7
0.8	2.3	2.2	4.1	4.4	6.2	8.0
	1.4	2.4	3.1	4.7	5.9	13.
0.9	5.0	2.6	5.6	8.9	13	6.9
	2.9	5.8	7.4	8.7	11	25
1.0	2.3	5.8	15	18	27	43
	10	12	15	17	21	30
1.1	12	30	39	53	65	
	26	25	30	36	44	
1.2	35	22				
	49	106				

4.3 Temperature dependence

As mentioned in Chapter 2, one of the goals of this thesis was to disclose the temperature dependence of the absorption in liquid semiconductors. Toward that end, the absorption has been carefully measured as a function of temperature in the alloys from the lowest limit defined by the immiscibility to the maximum temperature available for the cell, around 500 °C. The temperature dependence can be most clearly seen by plotting the logarithm of the absorption vs. inverse temperature, for a given photon energy. In this way one obtains a family of curves which can be referred to as isochromes. Figures 4.18-4.20 show plots of $\ln \alpha$ vs. t for x = 0, .001 and .005, where $t=1000/T\ K^{-1}$. A linear relationship which results.

Now the fact that $\ln \alpha$ is proportional to t is not a new discovery. This is in keeping with the Urbach behavior alluded to for the amorphous semiconductors [52]. However, an illuminating behavior of the slope $\partial \ln \alpha / \partial t$ with photon energy was found, which is in contrast to that expected from an Urbach representation. To see this, first consider Equation (4.1). One cannot ignore the possibility that both α_1 and α_2 may have different temperature dependences. Therefore in an analysis of the effect of temperature on the absorption in the alloy, one must be careful to consider only the temperature dependence in α_2. Now the intercept α_1 has been identified with the absorption in the absence of Tl, or the

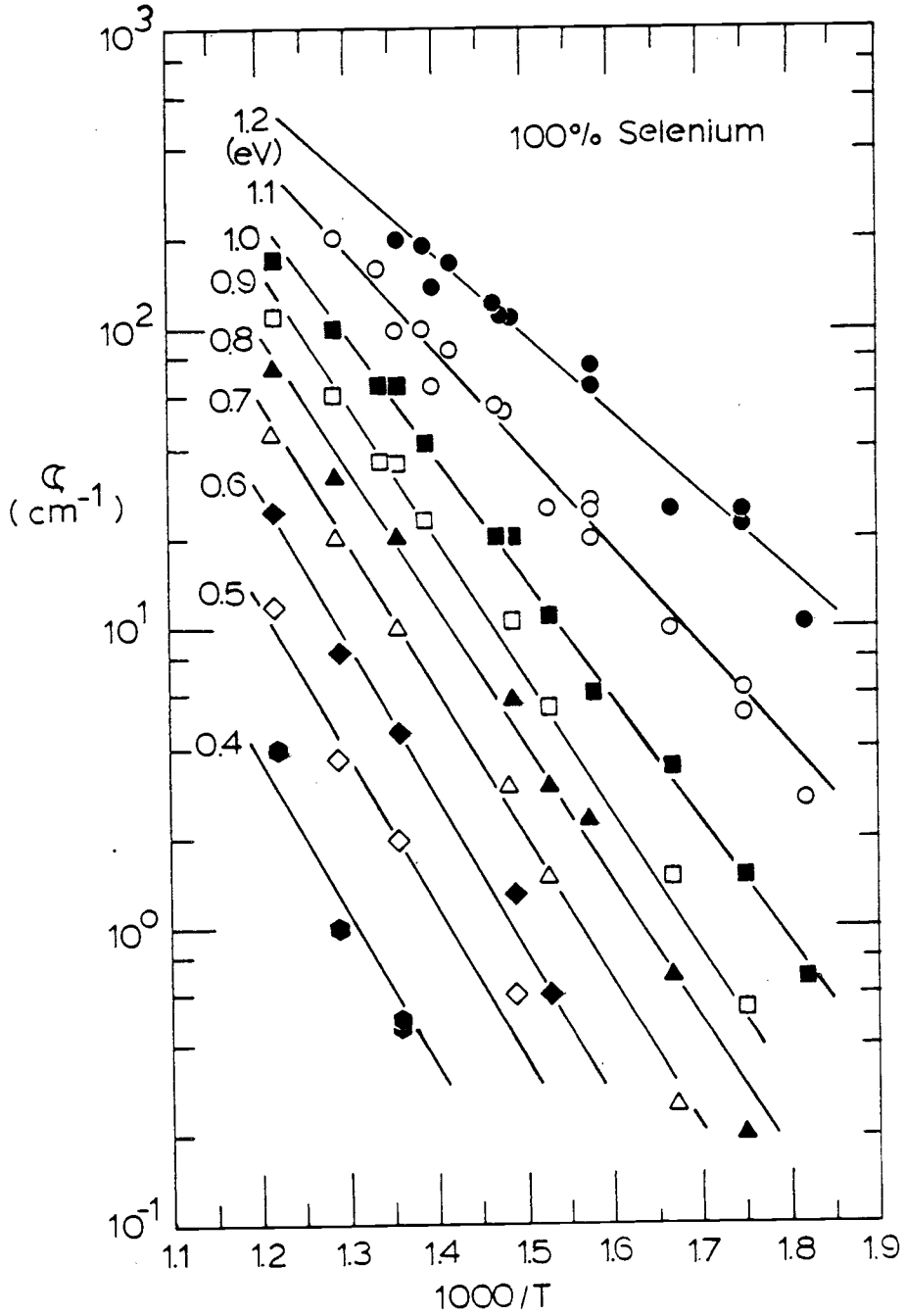

Figure 4.18 Absorption vs. 1000/T in liquid selenium for selected energies.

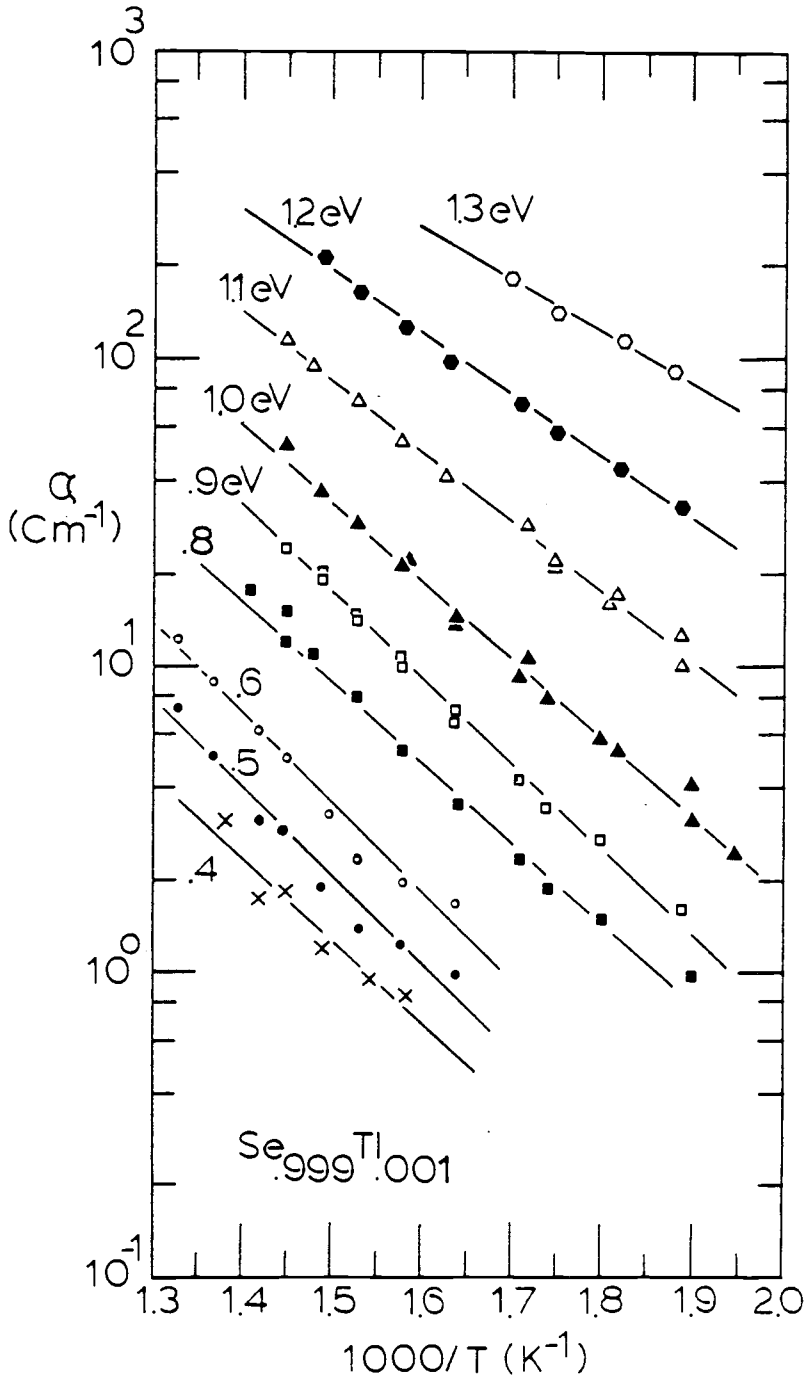

Figure 4.19 Absorption vs. 1000/T in $Se_{.999}Tl_{.001}$ for selected energies.

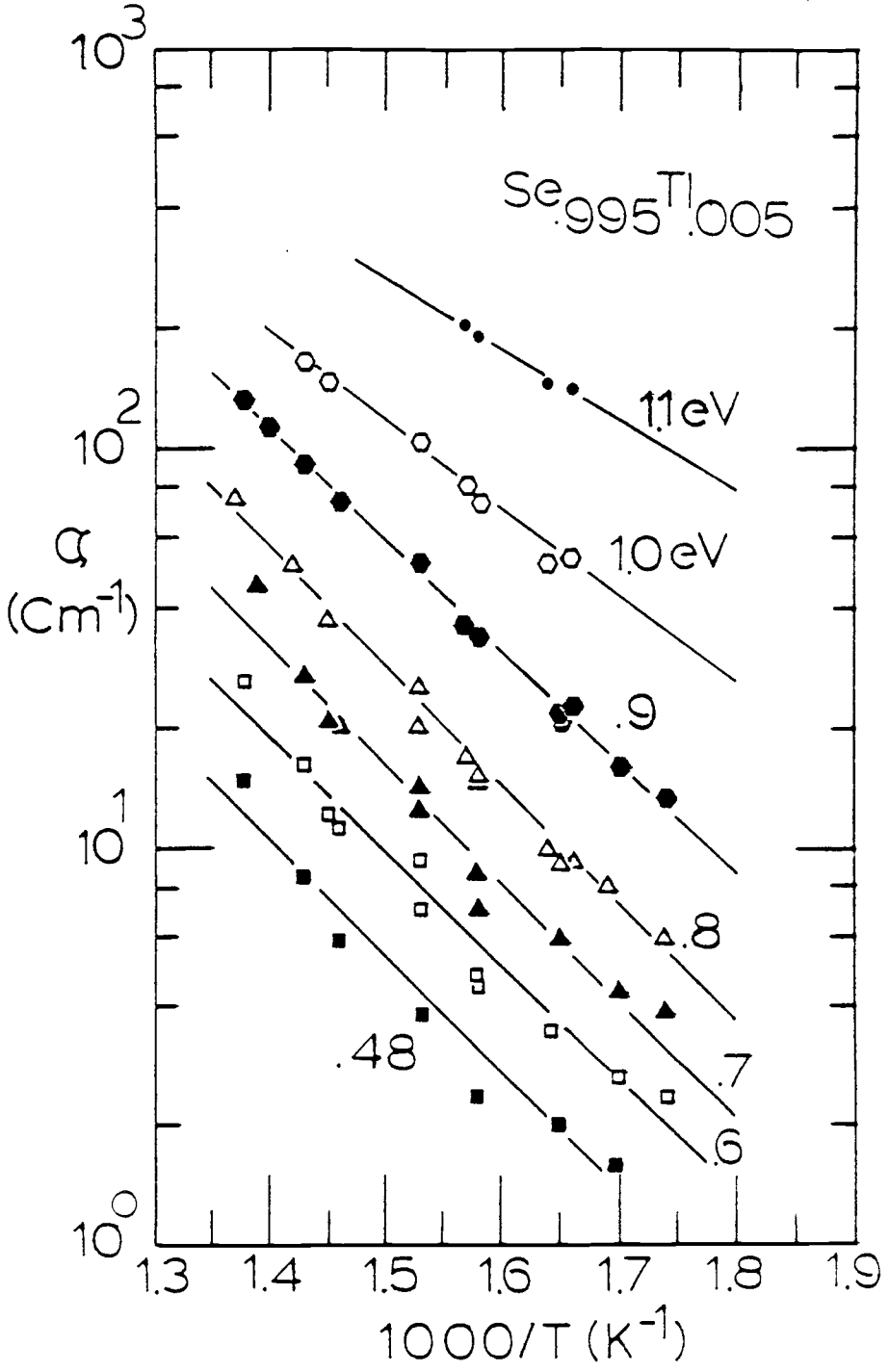

Figure 4.20 Absorption vs. 1000/T in $Se_{.995}Tl_{.005}$ for selected energies.

absorption in pure Se. Although this interpretation is open to question, it is qualitatively consistent with the data, and in any case α_1 represents a decreasing fraction of α_T as x increases. Consider then a quantity $\Delta\alpha$ defined to be:

$$\Delta\alpha(h\nu,T) = \alpha_T(h\nu,T) - \alpha_{Se}(h\nu,T). \qquad (4.2)$$

In this expression, α_T is defined as in Equation (4.1) and α_{Se} is the absorption measured in 100% Se at corresponding temperatures and energies. The temperature dependence in $\Delta\alpha$ is to be regarded as characteristic of the absorption due to the presence of Tl.

Now we are in a position to explore the temperature dependence of $\Delta\alpha$. Again, we consider the family of curves ln $\Delta\alpha$ vs. t for different energies. Representative plots for x=.001 and .007 are shown in Figures 4.21 and 4.22. The isochromes are linear in 1000/T as in α_T. Linear least squares fits to ln($\Delta\alpha$) vs. 1000/T have been made for all concentrations and the results are shown in Table 4.3 The upper listing in the table is the intercept; the lower the slope.

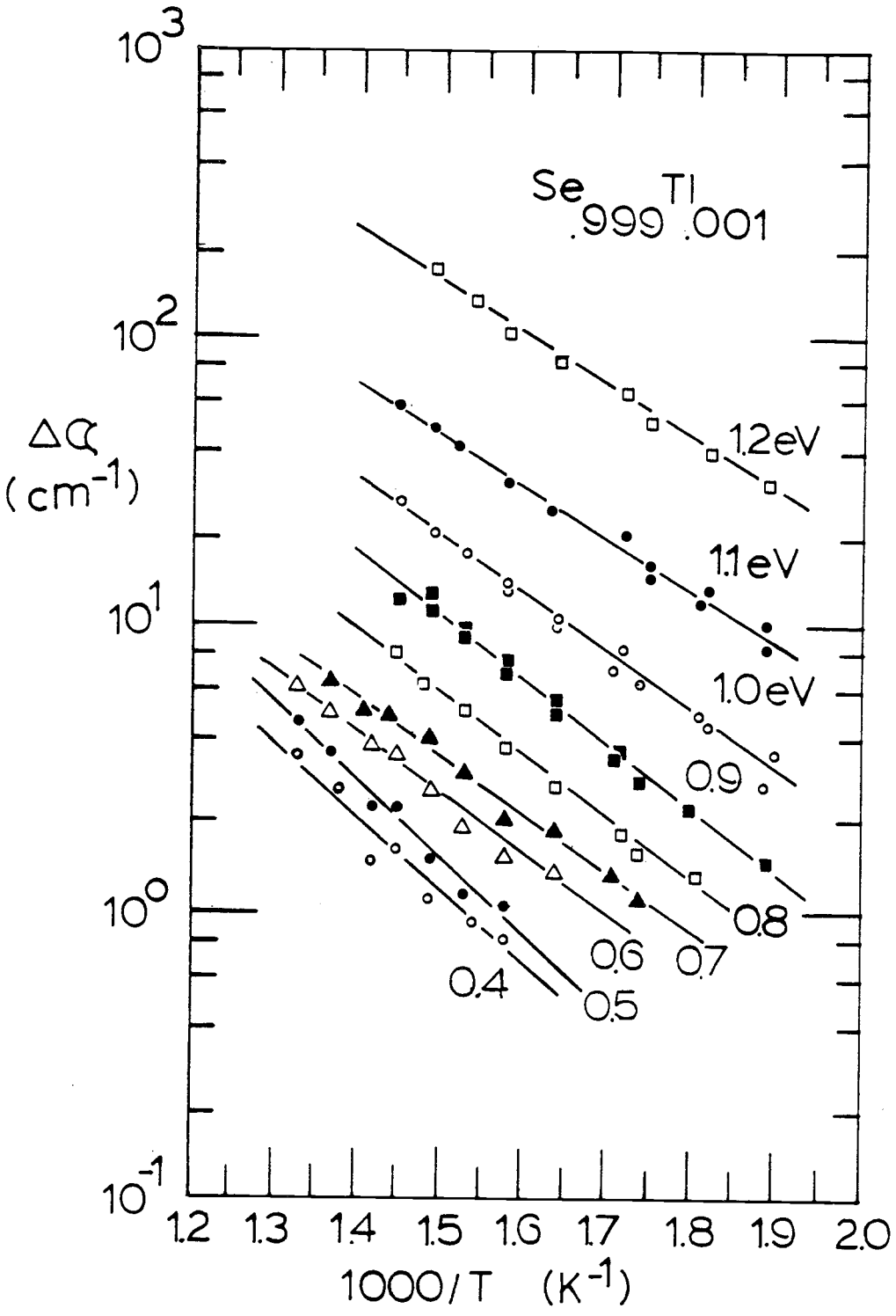

Figure 4.21 Absorption vs. 1000/T in $\Delta\alpha$ for $Se_{.999}Tl_{.001}$ at selected energies.

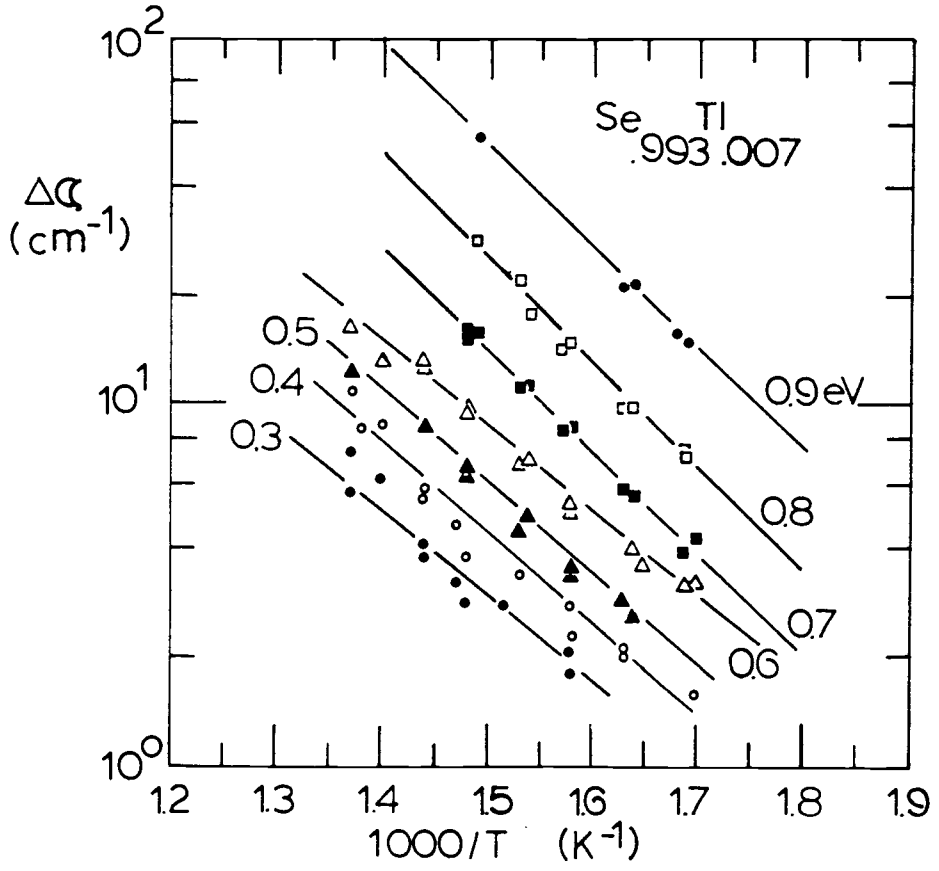

Figure 4.22 Absorption vs. 1000/T in $\Delta\alpha$ for $Se_{.993}Tl_{.007}$ at selected energies.

Table 4.3. Parameters from linear least squares fit of $\ln(\Delta\alpha)$ vs. t (t=1000/T). Upper value, intercept (dimensionless); lower value, slope (10^3K).

Photon Energies (eV)	Concentration (At fraction Tl)					
	.001	.002	.003	.005	.007	.009
0.4	7.9±1 -5.1±.7	9 ±1 -6±1	9±2 -6±1	13±1 -8.2±.8	10.1±.5 -5.8±.3	
0.5	9.7±.7 -6.2±.5	11±1 -7.1±.7	10±1 -6.1±.9		10.6±.4 -5.9±.3	
0.6	8.5±.6 -5.0±.4	9.1±.3 -5.3±.2	8.5±.5 -4.7±.3	13.4±.9 -7.5±.5	10.3±.3 -5.4±.2	12.1±.3 -6.4±.2
0.7	8.2±.3 -4.6±.2	9.0±.2 -5.0±.1	9.7±.5 -5.2±.4	13.4±.8 -7.2±.6	12.3±.3 -6.4±.2	11.5±.5 -5.6±.4
0.8	9.3±.3 -5.0±.2	11.0±.5 -5.9±.4	11.6±.4 -6.0±.3	13.7±.5 -7.0±.3	13.3±.8 -6.7±.4	12.1±.1 -5.7±.7
0.9	10.1±.3 -5.2±.2	11.5±.3 -5.8±.2	12.2±.4 -6.0±.3	13.1±.3 -6.1±.2	13.7±.7 -6.5±.3	10.5±.1 -4.2±.1
1.0	10.0±.3 -4.6±.2	11.5±.4 -5.4±.3	12.1±.3 -5.4±.2	11.6±.4 -4.7±.3		10.4±.1 -3.6±.1
1.1	10.0±.3 -4.1±.2	10.8±.3 -4.4±.2	12.4±.3 -5.1±.2	11.2±.7 -3.8±.4		
1.2	11.3±.2 -4.18±.1	10.3±.9 -3.6±.6				

Let us consider a quantity whose interpretation will be made precise later, but for now is defined by:

$$E_t(h\nu) = -[\partial(\ln\Delta\alpha)/\partial t]/11.7 \ \ (eV). \qquad (4.3a)$$

where 11.7=1/1000k. We shall be interested in the dependence of this quantity on photon energy. No systematic variation of E_t with concentration has been found. In fact, there is some scatter in E_t with concentration, which is within the uncertainty in the calculation of E_t. Therefore, let us take the average value of E_t with concentration at individual photon energies, and plot E_t vs. $h\nu$. This plot is shown in Figure 4.23. The error bars represent standard deviations in the average value of E_t for all concentrations.

A quantity similar to E_t may be calculated for absorption in 100% Se. This quantity, which we shall call E_{Se} is defined as in Equation 4.3a as:

$$E_{Se}(h\nu) = -[\partial(\ln\alpha_{Se})/\partial t]/11.7 \ \ (eV). \qquad (4.3b)$$

The values of E_{Se} have been calculated for absorption in 100% Se as

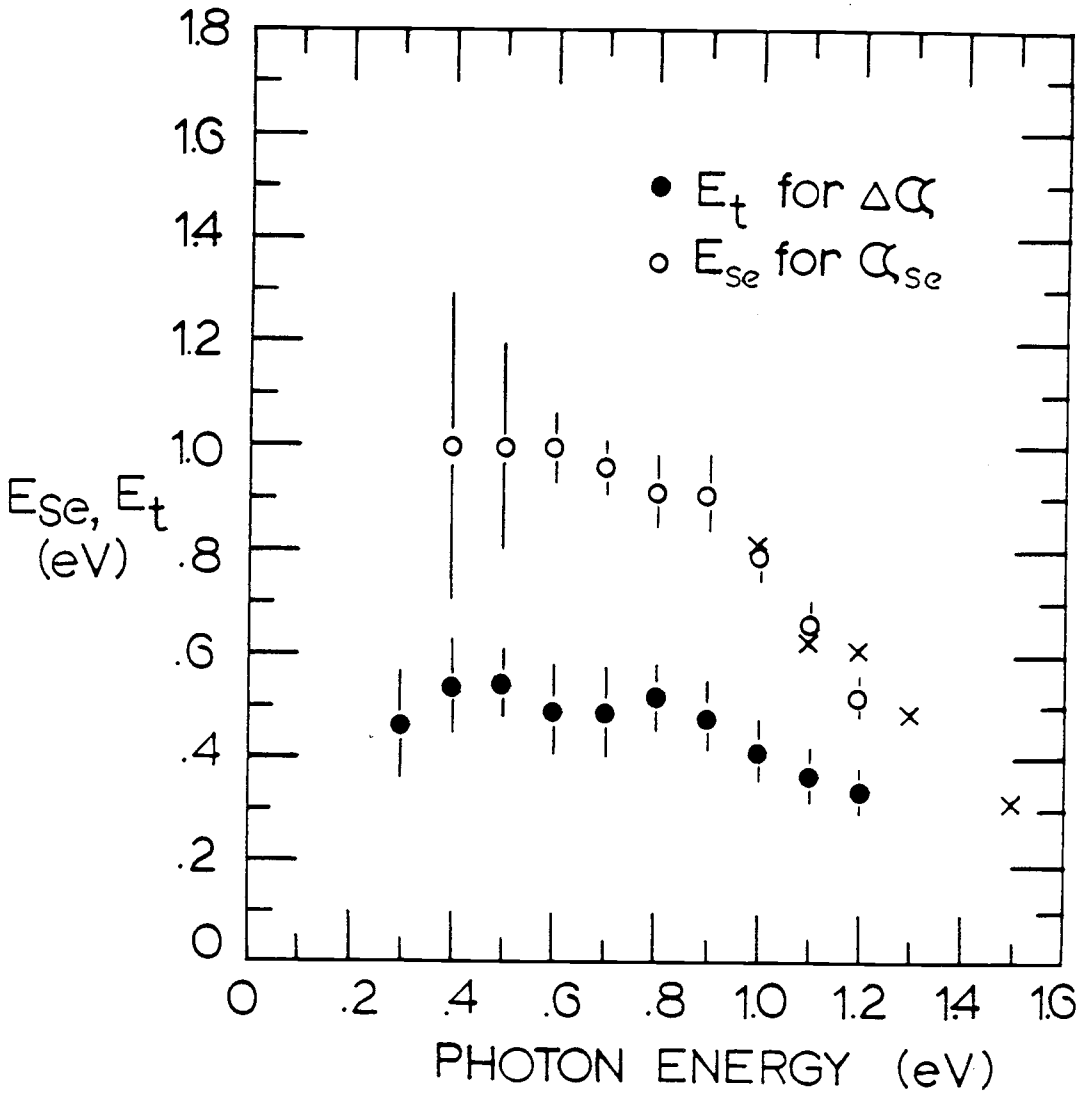

Figure 4.23 E_{Se} and E_t vs. photon energy. Solid symbols are E_t for the alloys averaged over all concentrations. Open symbols are for 100% Se taken from Figure 4.18. Symbols X are from the results of Ref. 19 (Fig. 2.5).

measured in this work (See Figure 4.18). These values are also shown in Figure 4.23. The corresponding values of E_{Se} have been calculated from the results of the absorption study of liquid Se by Siemsen and Fenton [19] (See Figure 2.5). These values are the symbols "X" in Figure 4.23.

Two distinct regions can be observed in Figure 4.23. First, there is a region $h\nu \lesssim .9$ eV for which E_t and E_{Se} can be considered constant. This constant value is about .5-.53 eV. The corresponding value of E_{Se} is about 1 ev. There is also a second region for $h\nu \gtrsim .9$ eV in which E_t is decreasing only slightly for the alloy, but E_{Se} decreases strongly.

Note *en passant*: E_t for $\partial\alpha/\partial x$ has been calculated using another technique. First $\partial\alpha/\partial x$ was calculated by a least squares fit and the parameters listed in Table 4.2 were produced. Then $\ln(\partial\alpha/\partial x)$ vs. t was plotted and the slope calculated. Although this method involves the use of quantities which have greater uncertainty, the values of E_t obtained in this way were found to be consistent with those calculated from $\Delta\alpha$.

In the past, exponential absorption edges have been said to follow the Urbach rule. Let us examine the parameter E_t and compare it to the slope of $\ln \alpha$ vs. t expected from an Urbach form (See Section 1.2). Consider the Urbach equation [52,55]:

$$\alpha_U(h\nu,T) = A\cdot\exp[\sigma(h\nu-E_0)/kT] \; . \qquad (4.4)$$

This is the form of the Urbach absorption, where σ and E_0 are fitting parameters. Now calculate a quantity for the Urbach rule corresponding to E_t as defined above:

$$E_t(\text{Urbach}) = -[\partial(\ln \alpha_U)/\partial t]/11.7 \qquad (4.5)$$

$$= -\sigma(h\nu - E_0)$$

E_t(Urbach) is therefore linear in $h\nu$. One can see immediately the difference between E_t as obtained from the alloy and the slope obtained from an Urbach fit. E_t is found to be constant for $0 \lesssim h\nu \lesssim .9$ eV in the alloy, in direct contrast to the $\sigma h\nu$ behavior representative of the Urbach form. One cannot therefore regard the absorption for $h\nu \lesssim .9$ eV as being represented by an Urbach rule. The observations on the temperature and Tl concentration dependence can be combined and expressed in empirical equation:

$$\Delta\alpha(h\nu,T) = x \cdot \exp^{-E_t/kT} \alpha(h\nu), \qquad (4.6)$$

where $$\alpha(h\nu) \approx \exp[\gamma(h\nu - E_0)]. \qquad (4.7)$$

This equation is expected to be representative of the absorption for photon energies $h\nu \leq E_g/2$.

In the past, the absorption edge in liquid Se has also been represented by the Urbach form. However, from the temperature dependence of the absorption in Se, it was found that that E_{Se} can be considered constant below approximately 0.9 eV, in contrast to the Urbach rule. It is worth pointing out that until this investigation, no data existed on the absorption in liquid Se below 0.6 eV, due to the IR cutoff of fused silica windows used in the absorption studies. It was, therefore, not unreasonable for previous investigators to interpret the E_{Se} slope as decreasing with $h\nu$. The present results indicate that in the region less than 0.9 eV, E_{Se} can be considered constant, similar to the situation in the alloy.

4.4 Summary of experimental results

Let us summarize the results of the experimental data:

1. The absorption is essentially exponential in $h\nu$ over the entire experimental range.
2. If there is a band gap shift to lower energies as the temperature or Tl concentration increases, it is relatively small.

3. The absorption can be written as the sum of two components, one of which is proportional to Tl concentration and the other essentially equivalent to the absorption in the absence of Tl.
4. The logarithm of the absorption for a given $h\nu$ is a linearly decreasing function of t, but the dependence on t is independent of $h\nu$ for $h\nu \lesssim 0.9$ eV, and so the absorption is not represented by the Urbach rule.

These conclusions represent the results of the experimental work. The interpretation of the quantity E_t is the only remaining task, and its interpretation will be combined with the calculation of the absorption in the ionic model (outlined in Section 2.3.5) to be described in detail in the following chapter.

5. THE IONIC MODEL

In this chapter the optical absorption coefficient is calculated for a liquid semiconductor containing a concentration C_i of ions, normalized to the number of atoms per unit volume. Because the system is electrically neutral, the number of ions of both charges per unit volume is $N_i=2N_aC_i$, where $N_a=2.7\times10^{22}$ cm^{-3}. This treatment is based on the Dow-Redfield [42,43] (D-R) theory of optical absorption in a uniform electric field with excitonic effects included. The reasons for rejecting the band shift model, the band tailing model, and the inaccurate representation of the absorption by an Urbach rule have been given in Chapter 4. The goal here will be threefold: (1) establish that the D-R theory gives the correct order of magnitude for the absorption, (2) establish that it gives the correct functional form of the absorption with the photon energy, and (3) establish that it gives the correct temperature dependence of the absorption.

The problem of optical absorption by excitons in a uniform field has been examined by several investigators, and these works are described in Ref. 59. We shall refer here to the development as given by Dow and Redfield. The absorption calculated by Dow and Redfield was derived for materials which can be characterized by a mean field $\langle F^2\rangle^{1/2}$, which is appropriate for field fluctuations due to optical phonons and ionic impurities in the low concentration limit. We shall be considering the absorption expected due to the presence of ions in a liquid

semiconductor in the D-R theory.

It is not the purpose here to take into account any physics not already considered in the D-R theory, such as nonuniformities of the electric field or distortion of the (assumed wide band) states due to the presence of large potential excursions near ions. Rather, a simple calculation is performed involving the averaging of the absorption $\alpha_{DR}(h\nu,F)$ (as derived by Dow and Redfield) over a distribution of electric microfields which is believed to be appropriate to a liquid containing ions. First the rationale for such a calculation is given.

5.1 Rationale for the ionic calculation

There is considerable evidence of the existence of charged atoms in liquid semiconductors. In particular, Rasolondramanitra and Cutler have obtained the density of ions for the systems $Se_{1-x}Te_x$ [11,14] for $.3 \leq x \leq .5$ and $Se_{1-x}Tl_x$ [11,15] for $.02 \leq x \leq .5$. We shall assume that ions are always present in a liquid semiconductor, that the concentration of ions is small ($C_i < 10^{-7}$) at low temperatures and near x=0, but that the concentration is thermally activated with an activation energy E_a, and can be characterized by a relation:

$$C_i = C_{i0} \exp^{-E_a/kT}. \qquad (5.1)$$

Because the ions are formed in pairs, the activation energy is equal to one-half the free energies of formation of the positive and negative ions. The prefactor C_{i0} is not easily specified, however, it is expected that to a good approximation, for the alloy system $Se_{1-x}Tl_x$, it is nearly equal to the concentration of Tl, $C_{i0} \approx x$. The actual value of C_{i0} may differ from x by a numerical factor and may also contain a factor involving the entropy. These unknown factors are expected to contribute an error to the calculation of less than an order of magnitude.

When ionic atoms are present, neutral atoms close to the ions will experience electric fields whose strength can be larger than 10^4 V/cm. From the reflectivity work of Fainschtein and Thompson [18], the dielectric constant of Se is approximately 4.2. The electric field at a distance r in Angstroms is then:

$$E = e/\epsilon r^2 = 3.4\times10^8/r^2 \quad (V/cm). \qquad (5.2)$$

Since the number of atoms per unit volume is $N_a = 2.7\times10^{22}$ cm^{-3}, there are about 700 neighboring atoms immersed in a field larger than 10^6 V/cm surrounding an ion. There is little doubt that when absorption occurs on these atoms, it is strongly affected by the presence of the field.

5.2 The Dow-Redfield model

The D-R theory was introduced in Chapter 2. It is a calculation of the optical absorption coefficient for optical transitions in the presence of a uniform electric field **E** (in the z-direction) and an excitonic interaction $-e^2/\epsilon r$. The wave functions are obtained by solving the Schrödinger equation in the relative coordinate system of the electron and hole. The Schrödinger equation is:

$$\left[\frac{-\hbar^2}{2\mu}\nabla^2 - \frac{e^2}{\epsilon r} - eEz\right] U(\mathbf{r}) = EU(\mathbf{r}). \qquad (5.3)$$

Now there is some question as to whether excitonic effects are important when a large electric field is present. This question was examined in detail by Dow and Redfield, and in particular, they calculated the absorption with the excitonic interaction (Coulomb interaction) included, and with the excitonic interaction "turned off." They found that with the Coulomb interaction turned off, the calculated absorption was at least three orders of magnitude smaller than when the interaction was included. This was found to be the case even when the fields were as large as 8.7×10^6 V/cm, showing that the exciton interaction is appreciable even up to very large fields. (For the case of Se, the dielectric constant ϵ=4.2, and the choice of m*=m gives an excitonic radius of 2.2 Å and excitonic Rydberg of .77 eV. In this case, the excitonic interaction is appreciable, and the D-R theory leads to a larger

absorption than the field-only interaction. A calculation of the absorption using the Franz-Keldysh result [36,37] rather than the D-R result was performed by this author, verifying that the absorption without excitonic interaction is, indeed, negligibly small for fields as large as 10^7 V/cm at photon energies $h\nu \leq E_g/2$.)

The results of the D-R calculation from Reference [42] can be summarized by the equation (for photon energies less than the band gap):

$$\alpha_{DR}(h\nu,F) = \frac{4\pi e^2 p^2}{m^2 c n \omega} \cdot |U_0(h\nu)|^2, \qquad (5.4)$$

where ω is the photon frequency, p is the momentum matrix element, and $|U_0(h\nu)|^2$ is related to the probability density of the electron-hole envelope wave function at zero wave vector [37,46,58]. This quantity involves the calculation of the wave function for a particular energy and field, which is fairly tedious, and this calculation must be performed numerically. This numerical calculation was performed by Dow and Redfield [40,41], and the results of their calculation of $|U_0(h\nu)|^2$ are shown in Figure 5.1. The abscissas in these graphs are in units of energy shift from the band gap divided by the exciton Rydberg energy (E_r). In the case of Se, ϵ=4.2, so that the exciton Rydberg is R=13.2eV/$(4.2)^2$=.77eV, and E_r=-(E_g-hν)/.77, where the photon energy and gap energy are in eV.

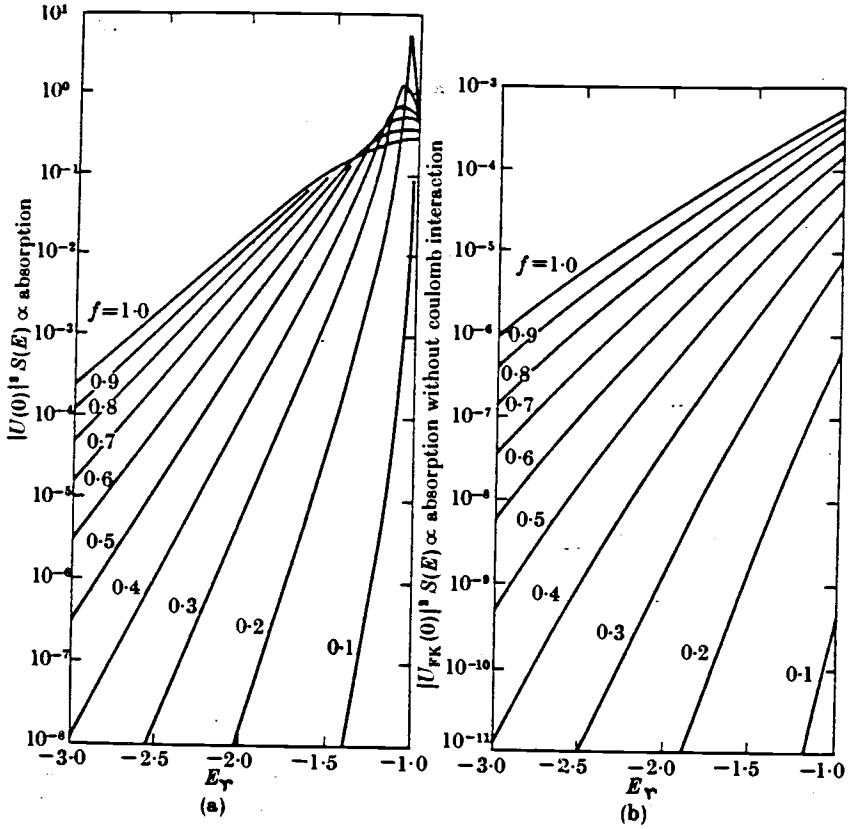

Figure 5.1 The absorption strength (a) with electric field and coulomb interaction and (b) with electric field only, corresponding to the Franz-Keldysh result. Abscissa is E_r shift as defined in the text. From Ref. 42.

The units of the ordinates are $1/Ra^3$, where a is the modified Bohr radius $a=a_0\epsilon$, and is aboout 2.2 Å. The individual curves are indexed by a parameter f which is proportional to the electric field. It is, in fact, the ratio of the potential drop across the excitonic radius to the exciton Rydberg, $f=|Eea/R|$.

There are two gross approximations used in the ionic model. The D-R theory assumes uniform fields, and in the present case the fields are nonuniform. This approximation will be poor at the largest values of the field. Also, the D-R calculation is based on the Elliot theory of optical absorption by excitons in a uniform field. The Elliot theory is developed in the Wannier representation of the exciton. As mentioned above, the modified Bohr radius is about 2 Å, and the excitonic Rydberg is .77 eV. This is not in the Wannier regime. Actually, in the present development, what we are doing is using a result which has been derived for a highly ordered system (a crystal with the full translational symmetry) and using it in the case of a highly disordered system. The D-R result is taken to be an approximation to the actual absorption in a nonuniform field, and in a disordered system, and in this case an order-of-magnitude calculation is all that is being attempted. As we shall see, the result is considerably closer to the observed absorption than one would expect.

5.3 Calculation of the absorption

The absorption is calculated by first considering the distribution of fields surrounding an ion. In the region surrounding any ion, there will

be a volume for which there will be some number of atoms experiencing a given field. This number will be the same for any other ion. The number of atoms experiencing a given field in the range between F and F + dF surrounding an ion will be:

$$n(F)dF = (dN/dF)dF = N_a(dV/dF)dF, \qquad (5.5)$$

where (dV/dF)dF is the volume per field.

We now assume that a pair of ions in the liquid is isolated in a volume $V_i=1/C_iN_a$. This will be valid in the limit of strong screening, where the concentration of ions is large, and the screening of a given ion involves essentially only one ion of opposite charge. The screening of ions in liquid semiconductors in the limit of high concentrations has been discussed by Cutler [56]. We allot to the volume V_i a number of atoms $N_S=N_aV_i=1/C_i$ for the purpose of calculating the influence of the ion field distribution on the optical absorption for atoms close to the ion, and far from any other ion. This will be accurate at the largest values of the field for which the atoms are representative, but inaccurate at the low field limit at r_i given by $4\pi r_i^3/3=V_i$. The field at this value of r_i is F_i and is a fair estimate of the $\langle F^2\rangle^{1/2}$ of Redfield.

Let us now define an absorption $\alpha^*(h\nu,F)=\alpha_{DR}(h\nu,F)/N_a$ which is the contribution per atom to the absorption coefficient at $h\nu$ and F, and

$\alpha_{DR}(h\nu,F)$ is the absorption as calculated in the D-R model. The contribution per atom per field to the absorption is then $(dN/dF)\times\alpha^*(h\nu,F)dF$. The total absorption due to the N_s atoms within the volume V_i is obtained by integrating the absorption per atom per field over the range of fields expected to be realizable:

$$\alpha_s(h\nu) = \int_{F_i}^{F_m} (dN/dF)\alpha^*(h\nu,F)dF \qquad (5.6)$$

$$= N_a \int_{F_i}^{F_m} (dV/dF)\alpha(h\nu,F)dF/Na, \qquad (5.7)$$

where Equation (5.5) has been used. The maximum field F_m is taken to be the field at the interatomic spacing r_n ($r_n \approx 3.5$ Å). That field is about 3×10^7 V/cm. We would not expect that any atom will experience a field larger in magnitude than this value. Now within a unit volume there are N_a atoms and the number of ions is $N_i=2C_iN_a$. Finally, then, we multiply by N_i to get the total absorption:

$$\alpha_i(h\nu,T) = N_i\alpha_s(h\nu) = 2C_iN_a\int_{F_i}^{F_m}(dV/dF)\alpha_{DR}(h\nu,F)dF. \qquad (5.8)$$

At this point we shall define a field in reduced units to simplify the calculations, which is $F=\epsilon E/e$. This field has units of $Å^{-2}$ and is related to the electric field by $E=1.44\times10^9\ F/\epsilon$ (V/cm). In terms of this field, the volume at a particular radius r is related to the field F at that radius as $V=4\pi/3F^{3/2}$. This is the volume (in units of $Å^3$) enclosed by the field F surrounding a particular ion. To obtain the volume per field, we must take the derivative of V(F) with respect to F. Therefore the derivative is $dV/dF=2\pi F^{-5/2}$. Putting in this and the value for $N_a=2.7\times10^{22}\ cm^{-3}$, Equation 5.8 becomes:

$$\alpha_i(h\nu,T) = 2.7\times10^{22}\,cm^{-3}\times10^{-24}\,cm^3\,Å^{-3}\times4\pi\times C_i$$

$$\times\int_{F_i}^{F_m}F^{-5/2}\alpha_{DR}(h\nu,F)dF,$$

$$= .34 C_i \int_{F_i}^{F_m} F^{-5/2} \alpha_{DR}(h\nu,F) dF , \qquad (5.9)$$

where now the field F in the integral is in $Å^{-2}$. This is the formula for the absorption and it remains to specify the absorption per field $\alpha_{DR}(h\nu,F)$.

$\alpha_{DR}(h\nu,F)$ is the absorption in a uniform electric field with an excitonic interaction included as calculated by Dow and Redfield [42,43]. It can be seen from the curves in Figure 5.1 that only incomplete information is available for the absorption strength, $|U_0(h\nu)|^2$. In order to do a complete calculation, values of the strength are required at other field values than those given. For values of f less than unity, an estimate of the strength may be given by rounding off an intermediate value of the field so that it will fall onto one of the curves on either side of it. This approximation is acceptable in view of the crudeness of the model itself.

For values of f larger than unity, there is no information available at all. This corresponds to fields larger than about 9×10^6 V/cm. We can, however, obtain an upper limit to the absorption by setting the strength equal to unity for f larger than one. This will result in larger values of absorption at the largest values of E_r (largest shifts from E_g), but will not change the calculation substantially at small values of E_r. We can

also obtain a lower limit to the absorption by simply terminating the integration at f=1. Both calculations have been carried out, verifying that the results differ only at smaller photon energies, and converge to the same values at higher energies. The results of this calculation are shown presently.

After putting in the values of the fundamental constants, we obtain a numerical value for the integral prefactor:

$$\alpha_i(h\nu,T) = (1.63\times10^6 \cdot C_i/h\nu) \int_{F_i}^{F_m} S(h\nu,F)\, F^{-5/2}\, dF. \qquad (5.10)$$

In this expression, $h\nu$ is in eV, F is in $Å^{-2}$, and $S(h\nu,F)$ is the dimensionless "absorption strength" to be taken from the curves in Figure 5.1.

5.4 The concentration and temperature dependence

The dependence of the absorption on Tl concentration and temperature comes about in a natural way through the concentration of ions C_i, as can be seen from Equation 5.1. According to Equation 5.1 and the comments following, we see that the calculated absorption will be proportional to the concentration of Tl. Such a proportionality is observed in the data for $\Delta\alpha$. Now re-write Equation 5.10 and insert the result C_i:

$$\alpha_i(h\nu,T) = [(1.63\times10^6 \cdot C_{i0}\cdot \exp^{-E_a/kT})/h\nu] \int_{F_i}^{F_m} S(h\nu,F)\, F^{-5/2}\, dF. \quad (5.11)$$

$$= [(1.63\times10^6 \cdot x\cdot \exp^{-E_a/kT})/h\nu] \int_{F_i}^{F_m} S(h\nu,F)\, F^{-5/2}\, dF, \quad (5.12)$$

where x is the thallium concentration.

We now make an identification of E_a. Because the only temperature dependence in the calculation is that in C_i, the calculated absorption itself will be thermally activated, with an activation energy equal to E_a. It was found (Chapter 4) that the temperature dependence of the absorption in the alloy was independent of the photon energy for energies less than 0.9 eV. It was therefore possible to write the absorption as (Equations (4.6) and (4.7)):

$$\Delta\alpha(h\nu,T) = x\, \exp^{-E_t/kT}\, \alpha(h\nu), \quad (5.13)$$

and

$$\alpha(h\nu) \approx \exp[\gamma(h\nu - E_0)]. \quad (5.14)$$

By comparing Equation (5.13) to Equation (5.12), we may identify the exponential thermal factors, and therefore make the identification $E_t \equiv E_a$. In other words, the temperature dependence in the measured absorption is due to the thermal activation of ions, as in the model. In the alloy, it was found that the activation energy was 0.5 eV for photon energies less than 0.9 eV, hence, we shall choose E_a=0.5 eV.

5.5 Results of the numerical calculation

Upon close examination of the numbers involved, one finds that the integral in Equation 5.12 converges very quickly for fairly large values of F_i. This is due to the decreasing product of the exponentially small values of $|U_0(h\nu)|^2$ and the power-law derivative dV/dF, and so is not surprising. It is found that the integrand becomes negligibly small at values of F≈.01, or the D-R f≈.4, which is an electric field strength of about 3×10^6 V/cm. This corresponds to a volume of integration that extends out to include only about a fraction 10^{-4} of the volume V_i. In other words, only a small fraction of the total atoms in the sample are contributing to the absorption, and most of those are atoms immersed in large fields fairly close to the ions (less than 10 Å).

In Figure 5.2 are shown the results of the calculations of α_i as a function of $h\nu$ for T=673 K, E_a=.5 eV, and x=.003, which is the dashed line

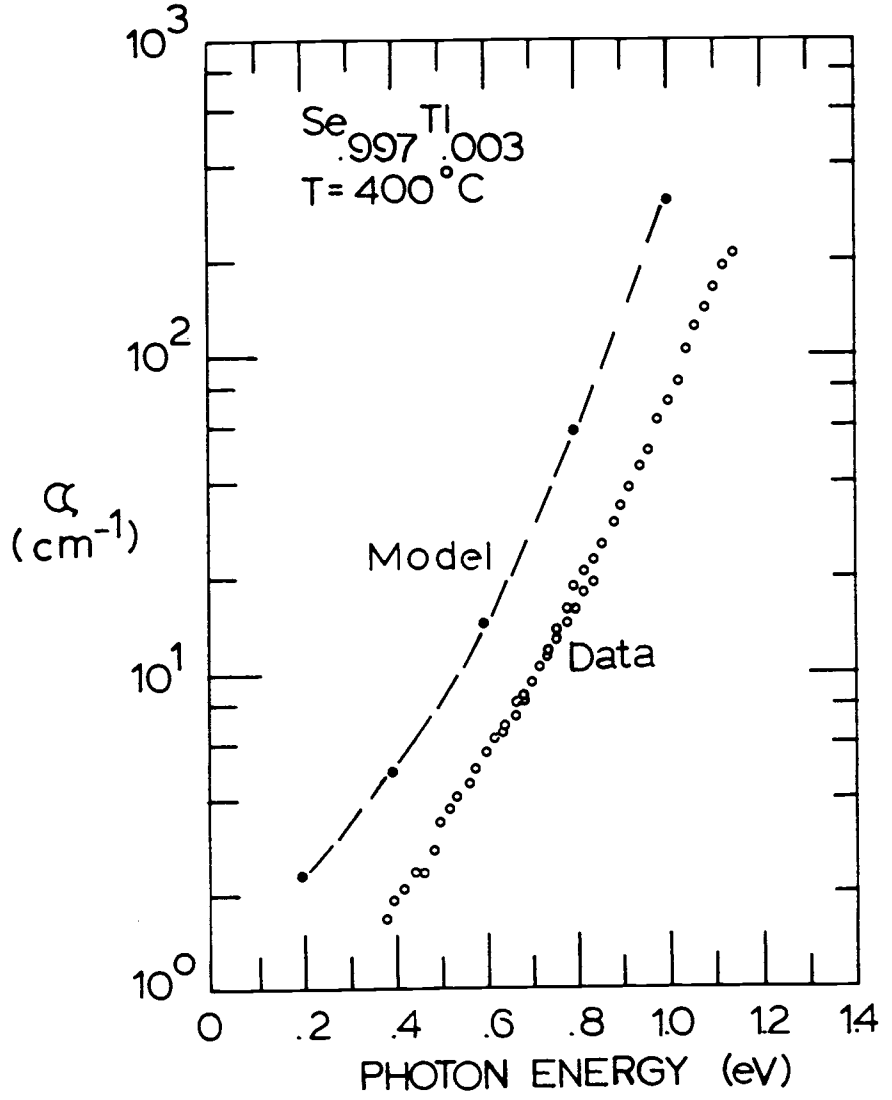

Figure 5.2 Absorption in the ionic model calculation for $Se_{.997}Tl_{.003}$ at 400 °C. Closed circles are model. Open circles here are data taken from Figure 4.6.

in the figure. The band gap has been chosen to be E_g=2.0 eV, the energy at which the photoconductivity turns on. (Recall the projected value for the gap energy from the data at $\alpha=10^5$ cm^{-1} is in agreement with this value.) In this calculation, the integration has been cut off at a maximum value of the field corresponding to the D-R f=1, or 9×10^6 V/cm. The curve marked "data" represented by open circles is the measured absorption in the alloy, $\Delta\alpha$, for x=.003, T=673K. As one can see, the close agreement in shape and the nearly correct magnitude are surprisingly good, in spite of the many crude approximations in the model.

It is of interest to compare the calculated absorption, independent of temperature and concentration, with the data. This is possible by considering the quantity (Equation 5.7):

$$\alpha_s(h\nu) = [\alpha_i(h\nu,T) \cdot \exp^{E_a/kT}]/x. \qquad (5.15)$$

This quantity may be compared to a corresponding quantity for the data obtained by dividing the measured absorption ($\Delta\alpha$) for a given concentration and temperature by the product of the concentration and the thermal term $\exp^{-E_t/kT}$, and averaging the result for a range of temperatures and all concentrations. These results are shown in Figure 5.3, where the lower curve is the result obtained from the data. The error bars on the data points reflect the standard deviation in the averaging. The upper two curves in the figure are the results of two

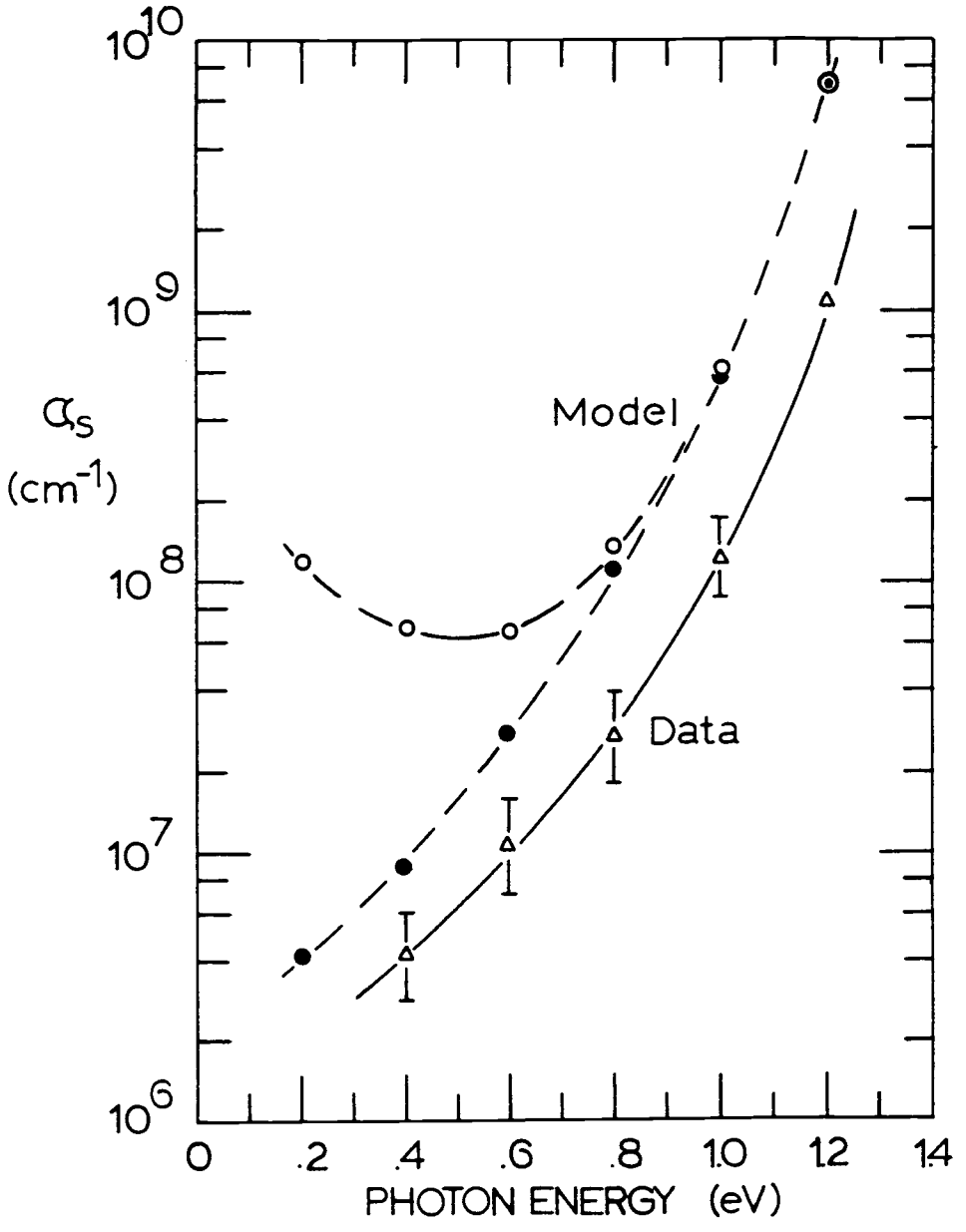

Figure 5.3 Concentration-independent absorption, $\alpha_s(h\nu)$. Upper curves are model (see text), and lower curve is from average over all data.

calculations of the temperature independent $\alpha_s(h\nu)$. The center curve represents the absorption which is obtained by cutting off the integration at a maximum field corresponding to the D-R f=1, or 9×10^6 V/cm. We shall refer to this as α_s(min). The highest curve is the absorption calculated by assigning a value to the absorption strength of unity above f=1. We refer to this as α_s(max). If results were available for the strength above f=1, the calculated absorption would lie on a curve somewhere in the region bounded by α_s(min) and α_s(max). Comparison of α_s with the curve derived from the data suggests that α_s(max) is a gross overestimation of the upper limit; the calculated absorption should be more closely represented by α_s(min).

5.6 Discussion

5.6.1 Uncertainties

The close agreement between the model caculation and the data is remarkable in view of the many crude approximations of the model. Of course the dependence on temperature and concentration was "built into" the model, and these results are not surprising. Also, the form of the strength, $|U_0(h\nu,F)|^2$, is exponential in the D-R model, and so the spectral shape of the calculated absorption is exponential as expected. However, the close agreement in magnitude is a result which is more than expected. Let us consider the factors which are uncertain in the

model, and could lead to an uncertainty in the magnitude of the calculated absorption:

1. The dielectric constant, ϵ=4.2, as obtained from the work of Fainchtein and Thompson, may be uncertain by 5%.
2. The reduced mass, μ, which has been taken to be $\mu=m_0/2$.
3. The momentum matrix element, p, which has been taken to be $\hbar/r_n$.
4. The identification $C_{i0}=x$.
5. The value of E_a=.5 eV.
6. Rounding off the D-R f to lie on one of the given curves.
7. The assumption of uniform fields.
8. The calculation is based on the absorption in the Elliot theory, which assumes wide band states for the initial and final states of the electron, when in fact, either or both states can be localized.
9. Cutting off the integration at a maximum field corresponding to the field at the interatomic spacing.

Of the above factors, the first five listed should contribute an uncertainty of less than an order of magnitude. Choice of the static dielectric constant ϵ is questionable at a field and radius corresponding to the interatomic distance. Using the static dielectric constant is at

best a gross simplification. The choice of E_a=.5 eV has an uncertainty of ±.1 eV. This leads to a multiplicative uncertainty of 5.6.

The rounding off of the D-R field f will lead to an overestimation of the strength when f is larger than half the distance between two of the curves and to an underestimation when f is smaller than half the distance. Both should occur equally, and so the effect may cancel, but this is not certain.

The D-R result has been derived for uniform fields. In the present situation, the field surrounding the ion has spherical symmetry. It is not certain what the effect of this nonuniformity is on the overall result, but we can say that the effect will be greater at larger values of the field, which corresponds to absorption on atoms closer to the ions. Now the number of atoms decreases as the distance from an ion decreases, so this tends to diminish the effect.

As mentioned earlier, the D-R result is based on the Elliot theory of optical absorption by excitons. The Elliot theory is appropriate for excitons in the Wannier representation, and that representation cannot be justified in the present case. However, we have obtained a result in the ionic model which is in good agreement with the experimental observations. Either this result is very fortuitous, or the exponential tailing (due to the combined effects of the electric field and the coulombic interaction) is preserved in the disordered state. Dow and Redfield comment [42,43] that it is the coulomb interaction which changes the $\exp(h\nu-E_g)^{3/2}$ (characteristic of the Franz-Keldysh or

field-only effect) to $\exp(h\nu-E_g)$ in the absorption coefficient. Perhaps the disorder alone is enough to relax the 3/2 power in the photon energy, but as noted earlier, the Franz-Keldysh (field-only) result is too small in magnitude to explain the absorption. It is difficult to offer any explanation which justifies the use of the ordered result in a highly disordered system such as a liquid semiconductor.

The effect of localization on the calculation is hard to determine. It is expected that states close to an ion will be strongly perturbed, and that they will become localized. The degree of localization is unknown. For initial and final localized states which are on different atoms, the wave functions will have a smaller overlap, and so the interband matrix element p will be smaller. Because the theory of localized states in disordered systems is not well developed, it not possible to say anything more about this particular question.

Cutting off the integration at a maximum field F_m corresponding to the interatomic distance may not be a poor approximation. This can be seen by considering the diagram in Figure 5.4, which shows the energy levels at a typical location in the semiconductor. The length scale here is about 100 interatomic spacings, total. The valence and conduction energies, which are normally flat in space are depicted by horizontal lines. The ions are expected to give rise to potential excursions as shown by the curvy lines.

We do not know the exact location of the Fermi energy. However, it is a fair assumption that it is near mid-gap. In this case, all the

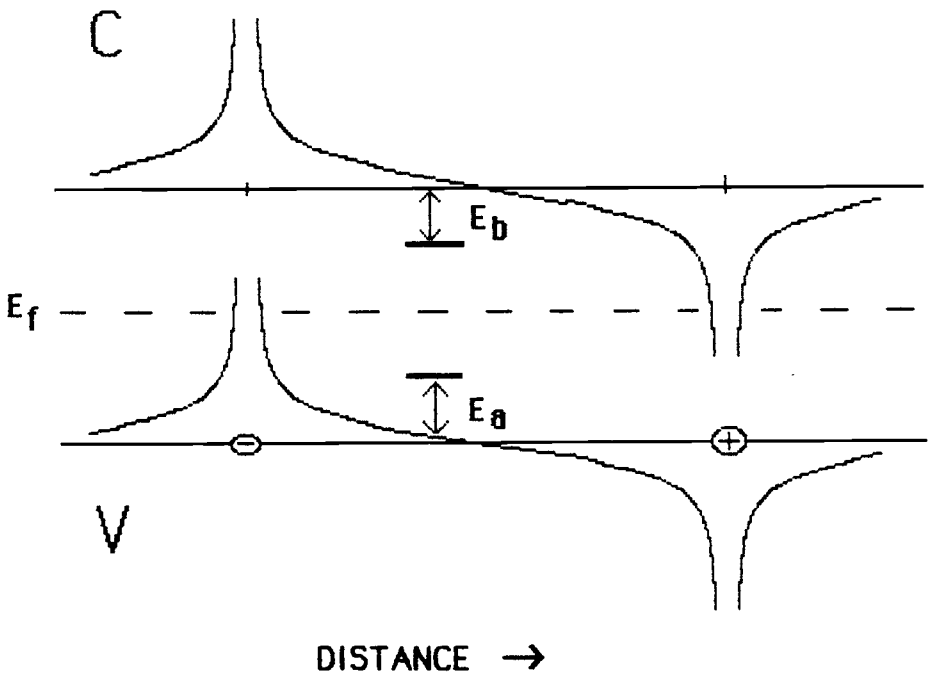

Figure 5.4 Energy levels at a typical location in the semiconductor. C and V refer to the conduction and valence bands. Horizontal lines show levels in the absence of fields. Curvy lines are potentials resulting from the ions. A likely position of the Fermi level is shown by a dashed line. E_a and E_b are two possible initial and final electronic state energies. The length scale is of the order 100 interatomic spacings.

valence states far from the ions and most of the states pushed upward in energy close to the negative ion will be occupied. However, there are a few states very close to the ion above E_f which are unoccupied, and will not be initial states of the optical transition. Therefore, there will be a cutoff radius (corresponding to a cutoff field F_m) for which states will not contribute to the absorption. In this regard it is not unreasonable to cut off the integration in F. The integration in the model (Equation 5.12) has been cut off at a value of F corresponding to the interatomic spacing (3.5Å), and at this field, the electrostatic energy is .98 eV .

5.6.2 Implications of the ionic model

There are several implications of the ionic model which must be reconciled with the experimental results. The first of these is that the activation energy is independent of the photon energy. However, in Figure 4.23 there are two distinct regions of behavior of E_t. The ionic model has been proposed to explain the absorption at energies $h\nu \leq E_g/2$. It is in this region of energy that the temperature dependence was in the form of a thermal activation and so the temperature effects could be separated from the spectral dependence. In the region $h\nu \geq 1.0$ eV, the data show a decreasing E_t as $h\nu$ increases. It is not possible to explain the decreasing E_t on the basis of absorption in a random field far from any ion. To see this, one can calculate the absorption expected from a

distribution of fields centered about the minimum field F_i, which should be representative of the regions far from any ion. Even for the maximum expected value for F_i, which is about 10^4 V/cm, the absorption is less than 10 cm^{-1} below 1.6 eV. This means that all the absorption at low photon energies and much of it at higher photon energies is due to transitions on atoms close to ions. This offers no explanation for the decrease in E_t above $E_g/2$.

The second implication of the ionic model is that if the Fermi energy is close to mid gap, for the initial state to be occupied and the final state to be unoccupied when $h\nu<E_g/2$, then the absorption must take place in a region close to a *pair* of ions. We can see this by considering the energy difference between E_g and $h\nu$, $E_1=E_g-h\nu$. Now $E_1 = E_a + E_b$, where E_a is the initial state energy of the electron on an atom close to the negative ion measured from the band edge, and E_b is the final state energy measured from the band edge, as shown in Figure 5.4. When $h\nu < E_g/2$, $E_1 > E_g/2$. Now when $E_1 > E_g/2$, since both E_a and E_b are less than $E_g/2$, neither of them can be equal to zero (neither can be an extended state). That is, if the initial state is on an atom close to an ion, the final state must be on an atom close to a counterion. Both states are localized. If we take $C_i \approx x\, e^{-E_a/kT}$, then if E_a=0.5 eV, $C_i \approx 10^{-6}$. The average separation distance is then about 200 Å. This is much too large

to be an appropriate tunnelling distance. In this case, the tunnelling distance is less than the average ionic separation distance, and transitions must take place between states close to ions which are separated by smaller-than-average separation distances.

There is a third implication of the ionic model which has to do with the concentration of Tl for the Se-Tl system. Rasolondramanitra and Cutler [15] have proposed that the dominant ionic species in the Se-Tl system is the D_s^+-D_m^- pair formation, where D_s^+ is the three-fold positively-charged Se defect and D_m^- is the Tl-Se^- diatomic ion. If the ionic mechanism is the D_s^+-D_m^- ion formation, then one expects the concentration of ions C_i to be proportional to $x^{1/2}$, where x is the Tl concentration. However, in the ionic model, C_i has been taken to be proportional to x.

5.6.3 The one- and two-ion hypotheses

The above implications can be reconciled quite naturally and satisfactorily by hypothesizing that absorption at $h\nu \leq E_g/2$ involves electrons on atoms close to a pair of oppositely-charged ions, and absorption at $h\nu \geq E_g/2$ also involves transitions on atoms close to a single ion. Let us see how these hypotheses fit the observations.

One of the problems with a single ion hypothesis for $h\nu \leq E_g/2$ is that the activation energy E_t is in disagreement with that obtained by

Rasolondramanitra and Cutler [15] from transport studies. Their value of E_a is about .17 eV. This value was obtained through an estimate of the dielectric constant for the $Se_{1-x}Tl_x$ alloys. If a correction is made for the dielectric constant at $x \leq .01$ (ϵ=4.2), the activation energy becomes E_a=.57 eV. In the present case E_t=0.5 eV. Now if we assume that the region $h\nu \leq E_g/2$ involves two ions, then the quantity E_t takes on a new definition:

$$E_t = 2E(C_i) - e^2/\epsilon r_p \qquad (5.16)$$

where $E(C_i)$ is the activation energy for the formation of the ions and the second term is the electrostatic potential energy of the ion pair. r_p is the interion separation distance. Putting in the values E_t=0.5 eV and $E(C_i)$=.57 eV, we obtain r_p=5.4 Å. This is a reasonable result for the separation distance.

When the separation of the ions is this small, it is possible for the tunnelling distance to be small, and both the initial and final states will be on atoms which are close to counterions. In this case, the initial state will be occupied and the final state will be unoccupied, even if the Fermi energy is near mid-gap (see Figure 5.4).

When the absorption involves states close to an ion pair, then to a first approximation, the absorption, $\Delta\alpha$, will be proportional to the

probability of finding a positive ion and negative ion close together, which, in turn, is proportional to the square of the concentration C_i^2. Now C_i should go as $x^{1/2}$ as mentioned earlier, so C_i^2 and hence $\Delta\alpha$ are proportional to x. What we are saying here is that the factor $x \cdot e^{-E_a/kT}$ is not strictly the concentration of ions, but rather the square of the concentration of ions, which is related to the probability of finding a positive and negative ion close together.

In the region $h\nu \geq E_g/2$, we have seen that the quantity E_t decreases as $h\nu$ increases. This behavior can be explained by hypothesizing that in this energy region, the absorption is a mixture of absorption on atoms close to single ions and absorption on atoms close to ion pairs. In this region, one cannot separate the contributions from both types of absorption. However, the lowest value of E_t (obtained at the highest value of $h\nu$) gives an upper limit estimation of the activation energy of the formation of ions (an alternative to the derivation of the activation energy from transport studies). At $h\nu$=1.2 eV, E_t=.33 eV. If we use this as an estimation of $E(C_i)$ in Equation 5.16, we obtain a separation distance of r_p=21 Å. Although a bit high, this result is not unreasonable.

The single-ion hypothesis above $h\nu=E_g/2$ implies that the absorption in this case will be proportional to $x^{1/2}$. Almost all of the data obtained in this thesis is for photon energies less than 1.2 eV, which is in the two-ion region. Therefore it is not possible to say

whether the $x^{1/2}$ behavior is in agreement with experiment. This question awaits further data in the region $E_g/2 \lesssim h\nu \lesssim E_g$.

The absorption coefficient has been derived in the ionic model assuming that the field distribution is well represented by the volume per field surrounding a single ion. In the two-ion region, the distribution of fields should be that for an extended dipole. Such a distribution has been calculated by this author, and in that case, the amount that the distribution differs from the single-ion distribution is not enough to seriously affect the calculation.

5.6.4 Implications for the case of liquid Se

The same arguments given for the one- and two-ion regions should apply in the case of liquid Se, when the ion pairs D_s^+-D_s^- are substituted for D_s^+-D_m^-. An equation similar to Eq. 5.16 can be written for the quantity E_{Se}:

$$E_{Se} = 2E(C_i) - e^2/\epsilon r_p. \qquad (5.17)$$

In this case, $E(C_i)$ is one-half the sum of the free energies of formation of the Se + and - ions. From Figure 4.23, E_{Se}=1.0 eV, and if we take the results r_p=20 Å obtained above, $E(C_i)$=.58 eV, and r_p=5.4 Å gives $E(C_i)$=.82

eV. From Figure 4.23 we see that the lowest value of E_{Se} is about .50 eV at $h\nu$=1.2 eV. These results are in fair agreement.

5.7 Conclusion

A calculation has been given of the optical absorption in the D-R theory of absorption in a uniform field with excitonic interaction. The absorption was derived by averaging the D-R result over a distribution of electric microfields surrounding an ion immersed in a material of dielectric constant ϵ=4.2. The total absorption was obtained by multiplying this result by the concentration of ions, which was assumed to be thermally activated. Thus, the resulting absorption is thermally activated with an activation energy related to the activation energy of the ions. Two regions of absorption were proposed to explain the two regions of activation energy. The region of low photon energy was explained to be associated with electronic excitation on atoms close to a pair of ions of opposite charge. The region of photon energy greater than half the band gap was explained to be a region involving a mixture of both excitations on atoms close to a single ion and to pairs of ions.

The excellent results obtained with this model make a strong case for the ionic interpretation. This model does not assume a shift of the band gap or a large density of tail states in the gap. The implications of the model, which are a thermal activation of the absorption, a proportionality to the Tl concentration in the case of Se-Tl alloys, and exponential absorption, are all in agreement with the data. Although some of

the approximations used in the model were crude, it is felt that the essential physics of absorption in liquid semiconductors with ionic defects is well represented by the model.

Finally, this model may provide a means of measuring the density of ionic defects in a liquid semiconductor. In Equation (5.7) we have defined the absorption per atom. The product of this quantity and the density of ions is the total absorption coefficient. If it were possible to measure both the density of ions and the absorption coefficient for a particular system, then it would be possible to calibrate the absorption and eliminate the uncertainties as outlined in Section 5.6. This would provide a way to measure the ionic concentration by measuring the optical absorption at low photon energies.

6. SUMMARY AND CONCLUSIONS

An infrared absorption cell has been developed for liquid semiconductors which can be used for measurements of absorption coefficients in the range $.1-10^3\ cm^{-1}$. The wavelength transmission range is limited only by the optical windows, which must be chosen for chemical compatibility with the semiconductor. Sapphire windows were used for this work, and that choice has allowed measurements down to .3 eV, below the previous .5 eV cutoff of fused silica windows. Because the cell was assembled with a clamping procedure using a graphite foil gasket, the cell thickness could be varied by changing the foil thickness, or by inserting a ceramic spacer to increase the cell thickness, or in the case of very thin cells, relieving one surface of the optical window. The cell thicknesses used were from 3500 μm to 50 μm.

Measurements were obtained of the optical absorption coefficient at the absorption edge for the liquid alloy system $Se_{1-x}Tl_x$ from the melting point up to 475 °C, and for x=0, .001, .002, .003, .005, .007, and .009. The absorption was found to be nearly exponential in the photon energy over the entire experimental range, from 0.3 eV to 1.2 eV. The absorption was found to be linearly increasing with concentration of Tl according to the empirical relation $\alpha_T(h\nu) = \alpha_1 + x\,\alpha_2$. The quantity α_1 was interpreted as the absorption in the absence of Tl, and this was found to agree with the absorption in 100% Se at corresponding temperatues and energies.

An excess absorption defined by $\Delta\alpha=\alpha_T - \alpha_{Se}$ was calculated and interpreted as the absorption due to the presence of Tl. This absorption was found to be thermally activated with an activation .5 eV for $h\nu \leq 0.9$ eV. The activation energy was found to be constant for $h\nu \leq 0.9$ eV, and to decrease above $h\nu \geq 1.0$ eV. It was argued that absorption at low energies is representative of absorption on atoms which are near ions pairs, and are therefore immersed in large electric fields, the absorption being shifted from the band gap as in the Franz-Keldysh effect. The effect is more pronounced at larger fields and low energies, which are appropriate for the regions closer to ions. The activation energy of the absorption is then related to the activation energy for the formation of ions, and so the absorption $\Delta\alpha$ is proportional to the probability of finding ions of opposite sign close together.

A simple calculation has been made of the absorption based on the Dow-Redfield theory of absorption in a strong electric field with excitonic effects. The Dow-Redfield result was averaged over the spherical distribution of the electric field surrounding an ion. The calculated absorption was then related to the concentration of ions. This model, although crude, was found to be sufficient to reproduce both the spectral shape and the temperature dependence. The magnitude of the calculated absorption was found to agree within the expected uncertainty.

Although the Dow-Redfield model has been suggested previously as a possible explanation for the exponential absorption edge in liquid semiconductors [16], there has been the question of the origin of the strong electric fields and how to represent such a field distribution. The present work suggests the origin of these fields in the fields surrounding ions and the distribution of fields follows naturally from this premise.

The ionic model satisfactorily explains the observed shift in the absorption edge with temperature and concentration (of metallic element in the case of alloy), and does not presuppose a shift of the band gap or a large density of states within the mobility gap. It provides a universal explanation of the exponential edge in liquid semiconductors where charged defects are present. It also provides a means of measuring the concentration of charged defects, if the absorption could be calibrated.

The activation energy of the formation of ions as obtained from thermoelectric studies should agree with that from the optical studies. There is one case where both the density of ions and the optical absorption have been measured for a single system. Rasolondramanitra and Cutler [11,14] have derived the densities of negatively charged ions for the system $Se_{1-x}Te_x$ at x=.3, .4 and .5, from transport studies. Also, Perron [1] has measured the optical absorption edge in the same alloys at x=.2, .3, and .5. However, only limited information was given by Perron at x=.5. It is unfortunate that the overlap of their data is not large enough to test the ionic model for agreement and to calibrate the absorption. A more thorough measurement of the absorption in the Se-Te system might

be fruitful in investigating the ionic model further. Also, a study of the thermoelectric behavior of $Se_{1-x}Tl_x$ at $x \leq .01$ would be very important, for it might provide the activation energy and density of ions to be compared with the values obtained herein.

BIBLIOGRAPHY

1. Perron, J. C., Doctoral Thesis, University of Paris (1969).
2. Richter, W., Renucci, J. B., and Cardona, M., Phys. Stat. Sol. 56, 223(1973).
3. Glazov, V. M., Chizhevskaya, S. N., and Glagoleva, N.N., Liquid Semiconductors, Plenum, New York (1969), p. 14.
4. See Reference 9., p. 178.
5. Edmond, J. T., Brit. J. Appl. Phys. 17, 979(1966).
6. Hodgson, J. N., Phil. Mag. 89, 735(1963).
7. Mott, N. F., and Davis, E. A., Electronic Processes in Non-Crystalline Materials, Clarendon, Oxford (1979).
8. Tauc, J., "Optical Properties of Amorphous Semiconductors," in Amorphous and Liquid Semiconductors, edited by J. Tauc, Plenum, London (1974).
9. Cutler, M., Liquid Semiconductors, Academic Press, New York (1977).
10. Brodsky, M. H., editor, Amorphous Semiconductors, Springer-Verlag, Berlin Heidleberg (1979).
11. Rasolondramanitra, H., Doctoral Thesis, Oregon State University, Physics (1983).
12. Kastner, M., Adler, D., and Fritzsche, H., Phys. Rev. Lett. 35, 1293(1975).
13. Vanderbilt, D. and Joannopoulos, J. D., Phys. Rev. B22, 2927(1980).

14. Cutler, M. and Rasolondramanitra, H., J. Non-Cryst. Sol. 61&62, 1097(1984).
15. Rasolondramanitra, H., and Cutler, M., Phys. Rev. B29, 5694(1984).
16. Rabit, J. and Perron, J. C., Phys. Stat. Sol. 65, 255(1974).
17. Tauc, J. and Abraham, A., Helv. Phys. Acta 41, 1224(1968).
18. Fainschtein, R., and Thompson, J. C., Phys. Rev. B27, 5967(1983).
19. Siemsen, K. J. and Fenton, E. W., Phys. Rev. 161, 632(1967).
20. Deprez, J., Rialland, J. F., and Perron, J. C., J. Phys. Lett. (France) 39, L142(1978).
21. Rialland, J. F. and Perron, J. C., Rev. Phys. Appl. (France) 11, 263(1976).
22. Zakharova, N. B., and Cherkasov, Yu. A., Sov. Phys. Sol. State 12, 1572(1971).
23. Tutihasi, S. and Chen, I., Phys. Rev. 158, 623(1967).
24. Hartke, J. L., and Regensburger, P. J., Phys. Rev. 139, 970(1965).
25. von Boehm, J., and Isomäki, H. M., Phys. Rev. B24, 6945(1981).
26. Ref. 7, p. 465.
27. Grison, E., J. Chem. Phys. 19, 1109(1951).
28. Caldwell, R. S. and Fan, H. Y., Phys. Rev. 114, 664(1959).
29. Trotter, D. M., Even, U., and Thompson, J. C., Phys. Rev. B17, 4004(1978).
30. Cohen, M. H., Fritzsche, H., and Ovshinsky, S. R., Phys. Rev. Lett. 22, 1065(1969).
31. Hindley, N. K., J. Non-Cryst. Sol. 5, 17(1970).

32. Ref. 7, pp. 11-12.

33. Stuke, J., J. Non-Cryst. Sol. 4, 1(1970).

34. Franz, W., Z. Naturf., 13a 484(1958).

35. Keldysh, L. V., Sov. Phys. JETP 34, 788(1958).

36. Tharmalingham, K., Phys. Rev. 130, 2204(1963).

37. Callaway, J., Phys. Rev. 130, 549(1963).

38. Moss, T. S., Burrell, G. J., and Ellis, B., Semiconductor Opto-Electronics, Butterworths, London (1973).

39. Pankove, J. I., Optical Processes in Semiconductors, Dover, New York (1971), pp. 46-52.

40. Redfield, D., Phys. Rev. 130, 914(1963).

41. Redfield, D., Phys. Rev. 130, 916(1963).

42. Dow, J. D. and Redfield, D., Phys. Rev. B1, 3358(1970).

43. Dow, J. D. and Redfield, D., Phys. Rev. B5, 594(1972).

44. Dow, J. D. and Hopfield, J. J., J. Non-Cryst. Sol. 8-10, 664(1972).

45. Dow, J. D. and Redfield, D., Phys. Rev. Lett. 26, 762(1971).

46. Elliot, R. J., Phys. Rev. 108, 1384(1957).

47. Ref 7, p. 278.

48. "Infrared Absorption Spectrometer for Liquid Semiconductors," F. Bell and M. Cutler, Oregon State Univ., Physics, submitted to Rev. Sci. Inst.

49. Grafoil is a trade name of Union Carbide Corp., Carbon Products Div., Niagra Falls, N. Y.

50. Hansen, M. and Anderkov, K., Constitution of Binary Alloys, 2nd. ed., McGraw-Hill, New York (1958).

51. Petit, R. B. and Camp, W. J., Phys. Rev. Lett. 35, 182(1975).

52. Ref. 7, pp. 275-283.

53. Ref. 7, p. 280.

54. Carroll, P. J., and Lannin, J. S., J. Non-Cryst. Sol. 35-36, 1277(1980).

55. Urbach, F., Phys. Rev. 92, 1324(1953).

56. Cutler, M., Philos. Mag. B49, 83(1984).

57. Recent analysis on 99.999% Se from ASARCO Chem. Corp.

58. Callaway, J., Quantum Theory of the Solid State, Academic Press, New York (1974), pp. 543-567.

59. Blossey, D. F. and Handler, P., "Electroabsorption," in Semiconductors and Semimetals, Vol. 9, Modulation Techniques, edited by R. K. Willardson and Albert C. Beer, Academic Press, New York (1972).

60. Bellissent, R., Nuc. Inst. and Meth., 199, 289(1982).

61. Kastner, M., in Proceedings of the 7th International Conference on Amorphous and Liquid Semiconductors, Edinburgh, edited by W. E. Spear, (1977), p 504.

62. Rabit, J. and Perron, J. C., Revue Phys. Appl. (France) 17, 277(1982).

APPENDIX

APPENDIX

EXAFS CELL

A modification of the optical cell described in Chapter 3 has been used by by this author for Extended X-ray Absorption Fine Structure Studies (EXAFS). In collaboration with Professor Daryl Crozier of Simon Frazer University, Burnaby, B.C. EXAFS mesurements on liquid semiconductors have been made with such a cell. Because the optical work demanded a thin, reusable cell of variable thickness, the design lended itself naturally to the con- struction of a thin x-ray cell suitable for the study of EXAFS in liquids.

The cell itself is a variation of the optical cell in design, differing in that hot-pressed boron nitride windows, one inch in diameter and three millimeters thick, were substituted for the infrared windows. The boron nitride was machined and polished on a turning lathe and then baked at 600 °C and 100μm vacuum to prevent outgassing during the experiment. Graphite foil gaskets (Grafoil) were used to confine the sample and seal the reservoir tip, as in the optical cell design.

In the EXAFS studies, a stainless steel heating block was used to clamp the cell together. It was noticed that at high temperatures, the cell experienced a good deal of corrosion due to the Se and Te vapors which leaked (there was not a hermetic seal). Work on the optical cell has shown that a good seal can be obtained by cementing the cell together using a mixture of Duco cement and acetone, which is applied to the gasket prior to assembly. A similar technique could also be used for

future EXAFS work. Also, the substitution of Inconel rather than stainless steel would eliminate the corrosion of the heating block.

The EXAFS measurements were conducted at the Stanford Synchrotron Radiation Laboratory in Palo Alto, California during the months of December, 1983 and March, 1984. Data was obtained on liquid Se-Te alloys at 50 and 70 per cent Te for temperature ranges up to 450 °C, at both the Se and Te k-edges. In addition, measurements were made on Te and glassy Se at room temperature and liquid nitrogen temperature. The analysis of these data is currently being carried out by Dr. Crozier's group at Simon Frazer University. Preliminary results show complementary agreement with the results of neutron scattering studies.